Science of the Total Environment 887 (2023) 164003

Contents lists available at ScienceDirect

Science of the Total Environment

journal homepage: www.elsevier.com/locate/scitotenv

Species selection determines carbon allocation and turnover in *Miscanthus* crops: Implications for biomass production and C sequestration

M.J.I. Briones [a,b,*], A. Massey [c], D.M.O. Elias [b], J.P. McCalmont [d], K. Farrar [c], I. Donnison [c], N.P. McNamara [b]

[a] Departamento de Ecología y Biología Animal, Universidade de Vigo, 36310 Vigo, Spain
[b] UK Centre for Ecology & Hydrology, Lancaster Environment Centre, Library Avenue, Bailrigg, Lancaster LA1 4AP, UK
[c] Institute of Biological, Environmental and Rural Sciences (IBERS), Aberystwyth University, Gogerddan, Aberystwyth, UK
[d] School of Biological Sciences, University of Aberdeen, King's College, Aberdeen AB24 3FX, UK

HIGHLIGHTS

- A better understanding of the C allocation dynamics in *Miscanthus* bioenergy crops is needed.
- We pulse-labelled ($^{13}CO_2$) intact plant-soil systems of three *Miscanthus* species for up to 190 days.
- *Miscanthus giganteus* and *M. lutarioriparius* allocated more photosynthates into above-ground biomass.
- *M. sinensis* crops transferred 30 % of fixed ^{13}C in its belowground biomass and emitted less CO_2.
- Careful selection of *Miscanthus* species may hold the success for reaching net GHG mitigation.

GRAPHICAL ABSTRACT

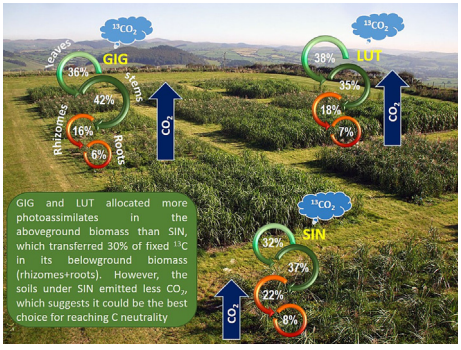

ARTICLE INFO

Editor: Elena Paoletti

Keywords:
$^{13}CO_2$ pulse labelling
Carbon storage
Miscanthus × *giganteus*
Miscanthus sinensis
Miscanthus lutarioriparius
Soil respiration

ABSTRACT

Growing *Miscanthus* species and hybrids has received strong scientific and commercial support, with the majority of the carbon (C) modelling predictions having focused on the high-yield, sterile and noninvasive hybrid *Miscanthus* × *giganteus*. However, the potential of other species with contrasting phenotypic and physiological traits has been seldom explored. To better understand the mechanisms underlying C allocation dynamics in these bioenergy crops, we pulse-labelled ($^{13}CO_2$) intact plant-soil systems of *Miscanthus* × *giganteus* (GIG), *Miscanthus sinensis* (SIN) and *Miscanthus lutarioriparius* (LUT) and regularly analysed soil respiration, leaves, stems, rhizomes, roots and soils for up to 190 days until leaf senescence. A rapid isotopic enrichment of all three species was observed after 4 h, with the amount of ^{13}C fixed into plant biomass being inversely related to their respective standing biomass prior to pulse-labelling (i.e., GIG < SIN < LUT). However, both GIG and LUT allocated more photoassimilates in the aboveground biomass (leaves + stems = 78 % and 74 %, respectively) than SIN, which transferred 30% of fixed ^{13}C in its belowground biomass (rhizomes + roots). Although less fixed ^{13}C was recovered from the soils (<1 %), both rhizospheric and bulk soils were signficantly more enriched under SIN and LUT than under GIG. Importantly, the soils under SIN emitted less CO_2, which suggests it could be the best choice for reaching C neutrality. These results from this unique large-scale study indicate that careful species selection may hold the success for reaching net GHG mitigation.

* Corresponding author at: Dept. Ecología y Biología Animal, Universidade de Vigo, 36310 Vigo, Spain.
E-mail address: mbriones@uvigo.es (M.J.I. Briones).

http://dx.doi.org/10.1016/j.scitotenv.2023.164003
Received 31 March 2023; Received in revised form 3 May 2023; Accepted 4 May 2023
Available online 9 May 2023

1. Introduction

Producing large amounts of biomass with very low fertilisation and management requirements (tillage is only required during the initial cultivation), together with high water and nitrogen-use efficiencies and being non-invasive have made of *M.* × *giganteus* the most common perennial bioenergy crop in Europe and USA (Clifton-Brown et al., 2008; McCalmont et al., 2017). In Europe, *M.* × *giganteus* has been widely used since 1983 for heat and electricity production (Lewandowski et al., 2000) and in the case of the UK, it is considered to have superior growth to other grasses in the current climate (RCEP, 2004). Consequently, it has been successfully used in several field trials where it was confirmed that it can retain high yields (10 t/ha yr^{-1}; Clifton-Brown et al., 2007) for at least 15 to 20 years (Dufossé et al., 2014; Shepherd et al., 2020). Due to this higher productivity and longevity, it appears to be not only a promising bioenergy crop, but also an efficient tool to combat climate change (Hastings et al., 2009; Hillier et al., 2009). Therefore, over the last decade it has been the focus of several studies to determine its ability to increase C accumulation in the soil (Amougou et al., 2012; Zatta et al., 2014; Poeplau and Don, 2014; Richter et al., 2015; Christensen et al., 2016; Robertson et al., 2017a; Nakajima et al., 2018; Holder et al., 2019; Ouattara et al., 2020; Al Souki et al., 2021) and to mitigate GHG emissions (Drewer et al., 2012; Zimmermann et al., 2012; Robertson et al., 2017b).

However, *M.* × *giganteus* also has disadvantages, such as a high sensitivity to very cold winter temperatures (Zub et al., 2012; Peixoto et al., 2015) and to drought (Cosentino et al., 2007). Furthermore, it can only be propagated vegetatively (through rhizome splitting), which leads to high establishment costs and low multiplication rates (Clifton-Brown et al., 2017, 2019). Vegetative propagation also results in low genetic diversity (Greef et al., 1997; Hodkinson et al., 2002), which makes it more difficult to improve through breeding programmes (Atienza et al., 2002) and more susceptible to soil-borne pathogens (Zub and Brancourt-Hulmel, 2010; Glynn et al., 2015).

Consequently, other *Miscanthus* species and varieties have become valuable sources of genetic material for intra- and interspecific breeding programmes (Lewandowski et al., 2016; Nunn et al., 2017; Clifton-Brown et al., 2019), with the selection largely focussing on obtaining higher yield, quality and resilience to abiotic stressors (Lewandowski et al., 2016). For example, *Miscanthus sinensis* despite having a lower aboveground biomass production compared to *M.* × *giganteus*, is more tolerant to water stress and hence, better suited for growing in drier climates (Ouattara et al., 2020). Similarly, *Miscanthus lutarioriparius* has been identified as yielding high biomass due to its high photosynthetic rate (Yan et al., 2012; Liu et al., 2013), but with lower heritability of traits such as cold and drought tolerance (Feng et al., 2022) that makes it more suitable for areas less exposed to frequent water shortages.

For their prospective for reaching C neutrality, however, a better understanding of the physiological traits driving the growth of *Miscanthus* species is needed. Perennial *Miscanthus* crops have the potential to sequester additional C in agricultural soils, allowing enough time, if established on lower C soils such as croplands or in marginal lands (Rowe et al., 2016; Wagner et al., 2019; Al Souki et al., 2021). Compared to other C_4 plants, root exudation and rhizodeposition appears to be low in *Miscanthus*, corroborating the idea that C dynamics in these plantations is dominated by recycling processes rather than by C stabilization (Robertson et al., 2017a; Holder et al., 2019; Zhang et al., 2018). Therefore, an alternative pathway for increasing C storage in the soil is through translocation of the C fixed through C_4 photosynthesis into rhizomes (Kuzyakov and Domanski, 2000) before harvest and further enhanced by the provision of soil C inputs from decomposing leaf litter and crop stubbles (Amougou et al., 2011). Indeed, the fact that *Miscanthus* stands of comparable age and with similar aboveground yield could differ in their rhizome and root C accumulation (Richter et al., 2015) has led to the suggestion that future studies should prioritize belowground biomass accumulation (Christensen et al., 2016).

By pulse-labelling intact plant-soil systems in the field with $^{13}CO_2$ for a short period of time (< 1 day), it is possible to determine how much C is allocated into the above- (leaves and stems) and belowground biomass (rhizomes and roots), retained in the soil and lost as soil respiration. Measurements of the ^{13}C natural isotopic abundance change in soils, which have exclusively grown C_3 photosynthetic crops, but then re-cultivated with C_4 *M.* × *giganteus*, have been used to estimate the stability of labile C inputs in the surface and subsoil (e.g., Dondini et al., 2009; Cattaneo et al., 2014; Zimmermann et al., 2012; Zatta et al., 2014; Richter et al., 2015; Christensen et al., 2016; Elias et al., 2017; Al Souki et al., 2021). The fate and dynamics of recently fixed C in other *Miscanthus* species has been seldom explored, with the exception of a few studies including *M. sinensis*, which confirmed that its C_4 photosynthetic pathway enhances soil C storage (Katsuno et al., 2010), although it accounted less than under *M.* × *giganteus* due to its lower rhizome biomass (Christensen et al., 2016).

Therefore, if we aim for climate change mitigation, effective selection of appropriate species will require to determine how C fixation, allocation belowground and turnover varies among species and hybrids, and to validate whether measurements of the total amounts of harvested aboveground biomass are a reliable proxy for estimating C sequestration. Therefore, in this study, we performed an in situ $^{13}CO_2$ pulse labelling experiment to investigate C allocation and turnover in three *Miscanthus* species, *Miscanthus* × *giganteus* (GIG), *Miscanthus sinensis* (SIN) and *Miscanthus lutarioriparius* (LUT), that are known to exhibit very different aboveground and belowground morphological traits and hence, with potential different pathways for above- and below-ground C transfer and allocation. Accordingly, *M. sinensis* plants are typically shorter (canopy height < 2 m) with a clumped base and multiple thin stems (Robson et al., 2013), *M. lutarioriparius* plants are taller with a spreading base with fewer, thicker stems (Yan et al., 2016), and the *M.* × *giganteus* hybrids show an intermediate phenotype in terms of the base and stem thickness (Robson et al., 2013). They can also be differentiated according to the growth habit of their rhizomes, and while *M. sinensis* forms dense centralised tufts made out of thinner stems (clumped), *M. lutarioriparius* has a non-tuft forming (rhizomatous growth habit), thick stemmed and lateral creeping rhizome (Chae et al., 2014), and *M.* × *giganteus* forms an intermediate type of rhizome (Lewandowski et al., 2003; Richter et al., 2015). Consequently, we anticipated (i) similar C assimilation rates due to their C_4 photosynthetic pathway (Elias et al., 2017), but different C retention in the aboveground biomass in the order of *M. sinensis* < *M.* × *giganteus* < *M. lutarioriparius* since this is linked to standing biomass, and (ii) a similar transfer of labile C to belowground plant tissues (rhizomes and roots) because this is directly related to phloem transport (Gavrichkova and Kuzyakov, 2017), but a higher retention of C in the belowground biomass under *M. sinensis* than in the other two *Miscanthus* crops due to its tuft rhizome system (Richter et al., 2015). Finally, we also predicted a greater accumulation of the new C in the soils under *M.* × *giganteus* in agreement with previous studies (Christensen et al., 2016) but counteracted by the losses through soil respiration as seen in other isotopic partitioning studies (Christensen et al., 2016; Robertson et al., 2017b).

2. Materials and methods

2.1. Experimental set-up

We used the Miscanthus genotype field trial established in 2010 at the Institute of Biological Environmental and Rural Sciences (IBERS), Aberystwyth, West Wales (52.4139′ N, −4.014′ W), where several genotypes have been planted in a randomised trial to investigate their suitability for bioenergy production in the UK, particularly in marginal lands (Clifton-Brown et al., 2008; Jensen et al., 2011). The long-term climatic data for the previous 30 years (1981–2010) from the nearest climate station (Gogerddan station: 52.43193′ N, −4.01929′ W; metoffice.gov.uk) indicates that the area has a hyperoceanic climate, with average maximum and minimum temperatures of 13.5 and 6.7 °C, respectively and total annual rainfall of 1074.7 mm (Köppen-Geiger classification: Cfb). Data from the meteorological station located in the field showed that, during the

investigated year (2013), the highest average temperature was 18.3 °C in July and the lowest was 4 °C in March, which was coincidental with the lowest rainfall values (Fig. S1).

The soil has been classified as a Denbigh soil, which is a well-drained, silt loam soil over rock and the underlying geology is a Palaeozoic slaty mudstone and siltstone (NSRI, 2008). The prior land use was for semi-improved perennial ryegrass and various grass breeding trials.

Three species of *Miscanthus* with widespread commercial use were selected for this experiment: (i) *Miscanthus sinensis* (Goliath) (SIN), a triploid intraspecific hybrid of *M. sinensis* (Purdy et al. 2015); (ii) *M. lutarioriparius* (LUT), a diploid variant of *M. sacchariflorus* that changed its status from being a subspecies to a separate species despite some remaining taxonomic controversy (Sun et al., 2010; Zhang et al., 2021); (iii) *Miscanthus* × *giganteus* (GIG), a sterile allotriploid hybrid of tetraploid *M. sacchariflorus* and a diploid *M. sinensis*. Second generation rhizomes were brought over from Germany for the IBERS breeding programme (i.e. they represent the parent material) and planted in nine experimental plots (N = 3 per species). Each plot was 25 m^2 (5 m × 5 m), randomly distributed across the field (Fig. S2) and with 49 plants of each species planted in each plot (7 × 7). Crop yield was measured annually between 2012 and 2014 by IBERS, with the results reported as tonnes per hectare.

2.2. Pre-pulse sampling of soils and plants

Aboveground (leaves, stems) and belowground plant biomass (rhizomes and roots) together with bulk soil samples (0–10 cm) were taken from each experimental plot before the pulse-labelling (Fig. S2). Three stems per plot were harvested and all leaves from each of them removed, dried and weighed. Samples of coarse roots and rhizomes were taken by digging with a shovel near the base of a randomly selected plant within a 2 × 2 m area designated for ^{13}C labelling and washed and dried prior to analysis. The dried weight of leaves and stems was summed and finally, multiplied by the number of stems per m^2 per plot to give the total standing biomass in g m^{-2} (dry matter).

Six 30 cm deep soil cores were collected using gouge augurs (Eijkelkamp Agrisearch Equipment, Giesbeek, Netherlands) with different diameters. Cores were taken from the soil surface between plants to avoid coring through rhizomes. Three of them (5 cm diameter) were used for bulk density and soil moisture content determinations. Fresh mass of the sample was recorded prior to air-drying (30 °C) and again after 10-days air drying. Air-dried samples were gently crushed and sieved to 2 mm. Stones and roots retained on the sieve were weighed and their volume determined by displacement of water in a measuring jug. This allowed for bulk density to be measured without stone content. A 15 g sub-sample of the air-dried, sieved soil was oven-dried at 105 °C for 24 h and re-weighed in order to derive total soil moisture content.

The remaining three cores (2.5 cm diameter) were horizontally sectioned into 3 depths: 0–10, 10–20 and 20–30 cm and each horizontal section was transferred to labelled bags and immediately frozen at −23 °C soon after collection. Vegetation samples were cleaned, oven-dried at 60 °C and cryo-milled (SPEX SamplePrep, Freezer/Mill 6770) to a fine powder prior to analyses. Bulked soils were freeze-dried and then sieved to remove stones while coarse and fine roots were picked out by hand, cleaned, oven-dried at 60 °C, cryo-milled and placed in glass sample vials. The remaining soil was ball milled (Fritsch Planetary Mill Pulviresette 5) to a fine powder ready for analysis.

Final dried samples of leaves, stems, rhizomes, roots and bulk soils were analysed for C and N contents (%) using an elemental analyser (LECO Truspec Micro, Michigan, USA) and for C isotopic analyses (see below).

2.3. $^{13}CO_2$ pulse labelling of Miscanthus plots

In each replicate plot, square ^{13}C pulse chambers were erected (2 m l, 2 m w, 3 m h) above the crop resulting in a total tent volume of 12 m^3. Aluminium scaffold was used to support plastic polythene film that allowed 90 % of photosynthetically active radiation (PAR) to enter the chamber.

Pulsing tents were sealed from the ambient atmosphere at 7:00 am on 26 July 2013 by using a continuous line of large sandbags (approx. 60 cm (l), 20 cm (h), 30 cm (w)) laid along the base of the enclosures on the tent skirt (Elias et al., 2017). CO_2 concentrations within the tents were initially monitored using a handheld infra-red gas analyser (IRGA) (EGM-4, PP Systems, Amesbury MA, USA) until photosynthetic CO_2 drawdown was observed. The ^{13}C pulse labelling started at ca. 08:20 h, once photosynthesis had commenced (identified by observing sub-ambient CO_2 concentrations within the pulsing tents), by introducing ca. 6 l of 99 % ^{13}C-atom enriched pure CO_2 (CK Gases, UK) in sequential batches over the course of ca. 2 h. The polythene tents were subsequently removed at ca. 11 am. In order to counter ambient air temperature increases within the chamber during the pulsing period, each was cooled using 3.9 kW water cooled, split air conditioner capable of air movement of 416 m^3/h (Andrew Sykes, UK). Additional air movement was facilitated by a tripod fan positioned opposite the air conditioning unit, within the pulsing chamber. One large 25 kWh diesel generator (located outside the experimental area) was used to provide power to all tents. During the ^{13}C pulse, air temperatures were regularly monitored inside the tent to ensure that temperature remained below 30 °C.

2.4. Soil CO_2 sampling

During the ^{13}C pulse, 20 ml gas samples were taken frequently via syringe and stored in 12 ml gas-tight exetainer vials (Labco, Lampeter, UK) for subsequent ^{13}C and CO_2 concentration analyses. Soil ^{13}C-CO_2 flux measurements were made one week prior to ^{13}C labelling and then at 4, 24, 48 h after labelling, followed by less frequent sampling on days 3, 4, 5, 7, 10, 14, 28, 56, 84 and 130 (14 time points × 3 chamber locations (2 within plot, one just outside) × 9 plots × 4 measurements per time point = 1512 gas samples; Fig. S2). The final gas sampling day was in December 2013. Two PVC static chamber gas collars (15 cm *d*, 10 cm *h*) were permanently installed into the soil to a depth of 2 cm below the surface at equal spacing within the ^{13}C pulsed area, while a third identical collar was positioned outside the experimental plot for periodic natural abundance control measurements required for the ^{13}C mass balance calculations. The chamber lid had a height of 20 cm and an internal diameter of 15 cm, and when sealed with the collar (inserted into the soil by 5 cm), the chambers had an internal volume of ~0.005 m^3 and a headspace volume of ~5 l. The chamber lids were sprayed with a reflective paint and fitted with a central septum for gas collection with a needle and syringe. Headspace gas samples (20 ml, 0.4 % of total chamber headspace volume) were taken using the static chamber method described by Anthony et al. (1995) at 0, 15, 30 and 45 min post enclosure and injected into 12 ml gas-tight borosilicate glass vials (Labco, Lampeter, UK) for subsequent GC analysis. At each gas sampling, measurements of soil moisture, soil temperature and air temperature were made. Three soil moisture measurements were taken around each gas sampling chamber with a handheld ML2Theta probe (Delta T Devices, Cambridge, UK) at a depth of 6 cm. Soil and air temperatures were taken at the beginning and end of each gas sampling around each chamber using a handheld temperature probe (Mini immersion thermometer, Testo Ltd., Alton, UK).

2.5. Post-pulse plant and soil analyses

At each gas sampling event (except 48 h, 4, 5 and 10 days) solid samples of leaves, stems, roots, rhizomes and bulk soils were taken from each experimental plot following the methodologies described above (n = 3 replicates × 10 time points). An additional sampling of plant tissues and soils took place at day 190 (03/02/2014). Green leaves were taken from the upper sections of the plant (upper leaves or "leaves") with the rest of the leaves and stems bulked together as one sample (stems + lower section leaves, "stems" henceforward). Only three plots out of nine had top leaves available for sampling on day 190 due to senescence: one GIG plot and two SIN plots.

As before, all solid samples were transferred to labelled bags and immediately frozen at −20 °C for processing. Vegetation and rhizome samples

were cleaned, oven-dried at 60 °C and cryo-milled (SPEX SamplePrep, Freezer/Mill 6770) prior to analyses. Bulked soils were freeze-dried and then sieved and ball milled (Fritsch Planetary Mill Pulviresette 5). Coarse and fine roots were picked out from the sieve, cleaned, oven-dried at 60 °C and then cryo-milled.

2.6. Gas sampling and isotopic analyses of respired CO_2, plant and soil samples

Gas samples were analysed separately for CO_2 concentration and $\delta^{13}C$ isotopic enrichment. 10 ml gas was removed from the glass sample vials via a syringe with a 2-way open/closed valve. These were attached to a 16-port distribution manifold feeding into a Small Sample Inlet Module (SSIM) and finally to a Picarro G-2131i Series CRDS (Cavity Ring Down) system where they were analysed automatically. A calibration gas sample (414 ppm, −9.98 ‰) was run after every 8 samples. 5 ml of the remaining sample gas was transferred to a 3 ml borosilicate glass sample vial (Labco, Lampeter, UK) and run on a PerkinElmer Autosystem XL Gas Chromatograph (GC) (PerkinElmer, Waltham, MA, USA) fitted with a Flame Ionisation Detectors (FID) operating at 130 °C and Electron Capture Device (ECD) operating at 360 °C. The GC was fitted with a stainless steel Porapak Q 50–80 mesh column (length 2 m, outer diameter 3.17 mm) maintained at 60 °C. Eight calibration gas standards (Air Products, Waltham on Thames, UK) were run per 32 samples and results were calibrated against these (Case et al., 2012).

Solid sample analysis was performed on a Costech ECS4010 Elemental Analyser (Costech Analytical Technologies Inc., CA, USA) coupled to a Picarro G-2131i Series CRDS analyser (Picarro Inc., CA, USA) via a split-flow interface using a method similar to Balslev-Clausen et al. (2013). Combustion gases were then vented through 1/16″ Swagelok stainless steel tubing into the Picarro Caddy split flow interface, which matches flow rates, before passing into the Picarro CRDS analyser for $\delta^{13}C$ analysis. Isotopic standards covering a representative range of $\delta^{13}C$ values were run during each analysis batch for instrument calibration.

2.7. Mass balance calculations and statistical analyses

Outputs from the Picarro $^{13}CO_2$ analyser were expressed in standard delta (δ) value notation ($\delta^{13}C$) [Eq. (1)], but converted to the atom % excess values for mass balance calculations [Eqs. (2) and (3)] as in similar previous studies (e.g. Elias et al., 2017; Briones et al., 2019). The atom % excess represents enrichment above the ^{13}C natural abundance values for each compartment (plant, root, rhizome, bulk soil and soil respiration) relative to the same samples taken before ^{13}C pulse labelling. Atom % excess was then calculated by subtracting the atom % enrichment of labelled samples from the corresponding atom % enrichment of natural abundance samples [Eq. (3)]:

$$\delta^{13}C_{sample} = \left(\left({}^{13}C/{}^{12}C_{sample)}\right) / \left({}^{13}C/{}^{12}C_{PDB}\right) \text{-}1\right) \times 1000 \quad (1)$$

$$\text{Atom } \% = \left(100 \times AR \times \left(\delta^{13}C/1000 + 1\right)\right) / \left(1 + AR \times \left(\delta^{13}C/1000 + 1\right)\right) \quad (2)$$

$$13C \text{ Atom } \% \text{ excess} = \text{atom } \%_{\text{pulse labelled sample}} - \text{atom } \%_{\text{background reference sample}} \quad (3)$$

where $^{13}C/^{12}C_{PDB}$ is the isotopic ratio of the standard material PDB, $^{13}C/^{12}C_{sample}$ is the isotopic ratio of a measured sample and AR is the absolute ratio of standard material (PDB) given as 0.0112372.

We used the slope of an OLS regression fitted to CO_2 concentrations measured at 0, 15, 30 and 45 min post enclosure to calculate CO_2 concentration change over time. Time series of CO_2 concentrations were quality controlled by discarding any with an $R^2 < 0.9$, and CO_2 fluxes (mg CO_2 – C m^{-2} h^{-1}) were calculated using Eqs. (4) and (5). Fluxes were partitioned into their ^{12}C and ^{13}C components using Eq. (2).

$$C_m = (C_v \text{ x } M \text{ x } P) / (R \text{ x } T) \quad (4)$$

$$F = (V \text{ x } C_{rate})/A \quad (5)$$

where C_m = Mass per volume concentration (μg CO_2-C/l), C_v = CO_2 concentration by volume (mixing ratio) (ppmv CO_2 - C), M = Molecular weight of CO_2, P = Barometric pressure (atm), R = Ideal gas constant defined as 0.08205746 l atm K^{-1} mol^{-1} and T = Air or chamber temperature at the time of sampling (K), F = Gas flux (mg CO_2 – C m^{-2} h^{-1}), V = Internal volume of the enclosure (m^3), C_{rate} = Change in gas concentration over enclosure period (mg CO_2 m^3/h) and A = area of collar enclosed soil surface (m^2).

The ^{13}C fluxes (μg m^{-2} h^{-1}) from the ^{13}C pulsed plots are a combination of pre-existing (old) natural abundance ^{13}C and enriched ^{13}C after labelling. Therefore, the ^{13}C excess flux was calculated using data from the chamber outside the ^{13}C pulsed plots as the background sample [Eq. (6)]:

$$^{13}C_{excess} \text{ Flux} = {}^{13}C_{\text{pulse labelled sample}}\text{flux} - {}^{13}C_{\text{background reference sample}} \text{ flux} \quad (6)$$

Normality and homogeneity of variances were checked using the Shapiro-Wilk test and the Levene's test, respectively, and data were log transformed ($\delta^{13}C$ signatures had to be log(−x) transformed, ^{13}C excess were log(x + constant) transformed and percentage data were arcsine [squareroot(x/100)] transformed) to improve variance homogeneity (Levene's test).

Analyses of Variance (ANOVA) was used to evaluate overall differences in abiotic conditions and in soil, plant and soil respiration samples between the three species (i.e. GIG, SIN, LUT) across the studied period. Repeated measures ANOVA was used to determine the influence of time, species and the interaction between these two factors on soil respiration rates and the absolute amount of ^{13}C excess in each of the plant sections, bulk soils and in soil respiration.

In addition, exponential decay functions were fitted to the isotopic values of plant tissue, soil and soil respiration samples measured on the different time points to compare the temporal changes in ^{13}C assimilation and translocation in the three species during the course of the experiment.

Finally, the interdependence of soil respiration rates and abiotic variables (air and soil temperature and soil moisture) was explored using linear correlations (Pearson correlation coefficient).

The data in Tables and Figures are presented as means ± S.E (n = 3). All statistical analyses were performed using SAS System Release 9.3 (SAS Institute Inc., Cary, NC).

3. Results

3.1. Pre-pulse crop parameters, plant and soil chemical properties and natural abundance delta values

During the investigated year *M. lutarioriparius* (LUT) produced the tallest plants, followed by *M. giganteus* (GIG) and *M. sinensis* (SIN) (Table 1). However, despite not being a tall-growing crop, GIG rendered the highest yield (Table 1).

Species identity did not affect gravimetric soil moisture contents, 30 % on average (Table 1). Similarly, there were no significant differences in bulk density values between the three *Miscanthus* species and on average were approximately 1 g cm^{-3} across the plots (Table 1). This is expected for a Denbigh soil (fine loamy/fine silty) which has extensive root growth.

Pre-pulse measurements of the vegetation indicated that leaves, stems and rhizomes had higher C contents than roots, with GIG showing the lowest values in its roots relative to the other C pools (Fig. 1a and Table 1). In contrast, most plant N was concentrated in the leaves of the three crops (Fig. 1b and Table 1).

The species identity of the plant crop had a significant effect on total soil C ($ANOVA_{SPECIES}$: F = 6.43, p = 0.0078) and total N concentrations ($ANOVA_{SPECIES}$: F = 4.90, p = 0.0182) and the soils under LUT stored higher amounts of these two elements, more so in the 10–20 cm soil layer (Table 1 and Figs. 1c,d). The lowest values were measured in the

Table 1
Crop parameters, plant and soil chemical properties and natural abundance delta values at the three *Miscanthus* treatments in the investigated year prior to the ^{13}C pulse-labelling experiment (mean ± S.E.; $n = 3$). Different letters indicate significant differences between *Miscanthus* species per parameter.

	Miscanthus × giganteus	*Miscanthus sinensis*	*Miscanthus lutarioriparius*
Vegetation			
Crop height 2013 (cm)	200.78 ± 6.27a	153.22 ± 0.61b	249.44 ± 1.67c
Crop yield 2013 (t/ha)	16.05 ± 1.10a	5.46 ± 1.08b	10.63 ± 1.73ab
Litter fall 2013/2014 (g m^{-2})	689.02 ± 108.38a	684.10 ± 130.78a	887.14 ± 131.94a
Leaves C content (%)	44.00 ± 0.49a	43.97 ± 0.19a	44.80 ± 0.18a
Stems C content (%)	42.10 ± 0.37a	42.18 ± 0.30a	42.90 ± 0.42a
Rhizomes C content (%)	42.99 ± 0.89a	39.20 ± 4.54a	43.72 ± 2.37a
Roots C content (%)	29.20 ± 4.48a	36.22 ± 1.69a	38.04 ± 0.88a
Leaves N content (%)	2.27 ± 0.02ab	1.87 ± 0.18a	2.43 ± 0.05b
Stems N content (%)	1.34 ± 0.16a	1.01 ± 0.10a	0.87 ± 0.07a
Rhizomes N content (%)	1.44 ± 0.33a	0.84 ± 0.04a	0.78 ± 0.17a
Roots N content (%)	0.88 ± 0.08a	1.12 ± 0.17a	0.83 ± 0.06a
$\delta^{13}C$ leaves (‰)	−10.34 ± 1.08a	−9.90 ± 0.91a	−12.34 ± 0.13a
$\delta^{13}C$ stems (‰)	−10.78 ± 0.63a	−9.45 ± 4.23a	−12.25 ± 0.18a
$\delta^{13}C$ rhizomes (‰)	−10.74 ± 0.31a	−10.87 ± 0.35a	−11.41 ± 0.34a
$\delta^{13}C$ roots (‰)	−13.74 ± 1.87a	−12.52 ± 0.57a	−12.65 ± 0.56a
Soil			
Moisture content 0–30 cm (%)	30.15 ± 2.59a	31.00 ± 1.38a	28.84 ± 1.33a
Bulk density 0–30 cm (g cm^{-3})	1.10 ± 0.06a	1.06 ± 0.03a	0.95 ± 0.07a
Total C content 0–30 cm (%)	3.08 ± 0.14a	3.12 ± 0.19a	3.96 ± 0.25b
Total C content 0–10 cm (%)	3.27 ± 0.06a	3.00 ± 0.35a	3.85 ± 0.14a
Total C content 10–20 cm (%)	3.39 ± 0.04a	3.50 ± 0.17a	4.23 ± 0.19b
Total C content 20–30 cm (%)	2.58 ± 0.22a	2.87 ± 0.39a	3.81 ± 0.80a
Total N content 0–30 cm (%)	0.34 ± 0.01a	0.35 ± 0.01ab	0.42 ± 0.03b
Total N content 0–10 cm (%)	0.35 ± 0.01a	0.36 ± 0.00a	0.40 ± 0.02a
Total N content 10–20 cm (%)	0.37 ± 0.01a	0.37 ± 0.02a	0.44 ± 0.01b
Total N content 20–30 cm (%)	0.29 ± 0.02a	0.32 ± 0.03a	0.42 ± 0.09a
$\delta^{13}C$ 0–30 cm (‰)	−26.03 ± 0.23a	−26.46 ± 0.29a	−26.81 ± 0.27a
$\delta^{13}C$ 0–10 cm (‰)	−25.80 ± 0.50a	−26.47 ± 0.64a	−26.18 ± 0.65a
$\delta^{13}C$ 10–20 cm (‰)	−26.51 ± 0.28a	−26.78 ± 0.70a	−27.21 ± 0.30a
$\delta^{13}C$ 20–30 cm (‰)	−25.77 ± 0.33a	−26.15 ± 0.20ab	−27.04 ± 0.28b

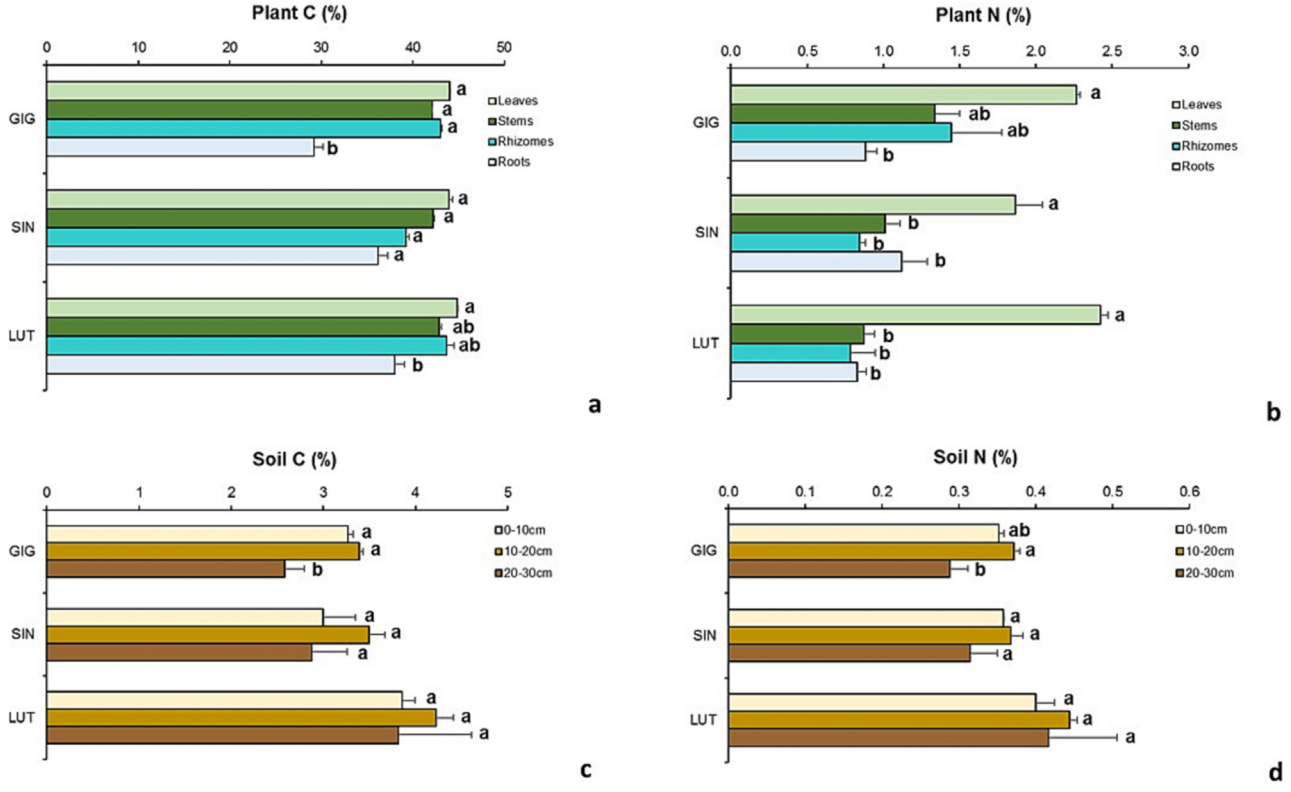

Fig. 1. Averaged (a) C and (b) N contents in above- and below-ground plant tissues and (c) soil C and (d) N contents measured at 0–10, 10–20 cm and 20–30 cm at the three *Miscanthus* treatments (pre-pulse). Error bars are S.E. and different letters indicate significant differences between soil depth per *Miscanthus* species (*Miscanthus × giganteus* (GIG), *Miscanthus sinensis* (SIN) and *Miscanthus lutarioriparius* (LUT)).

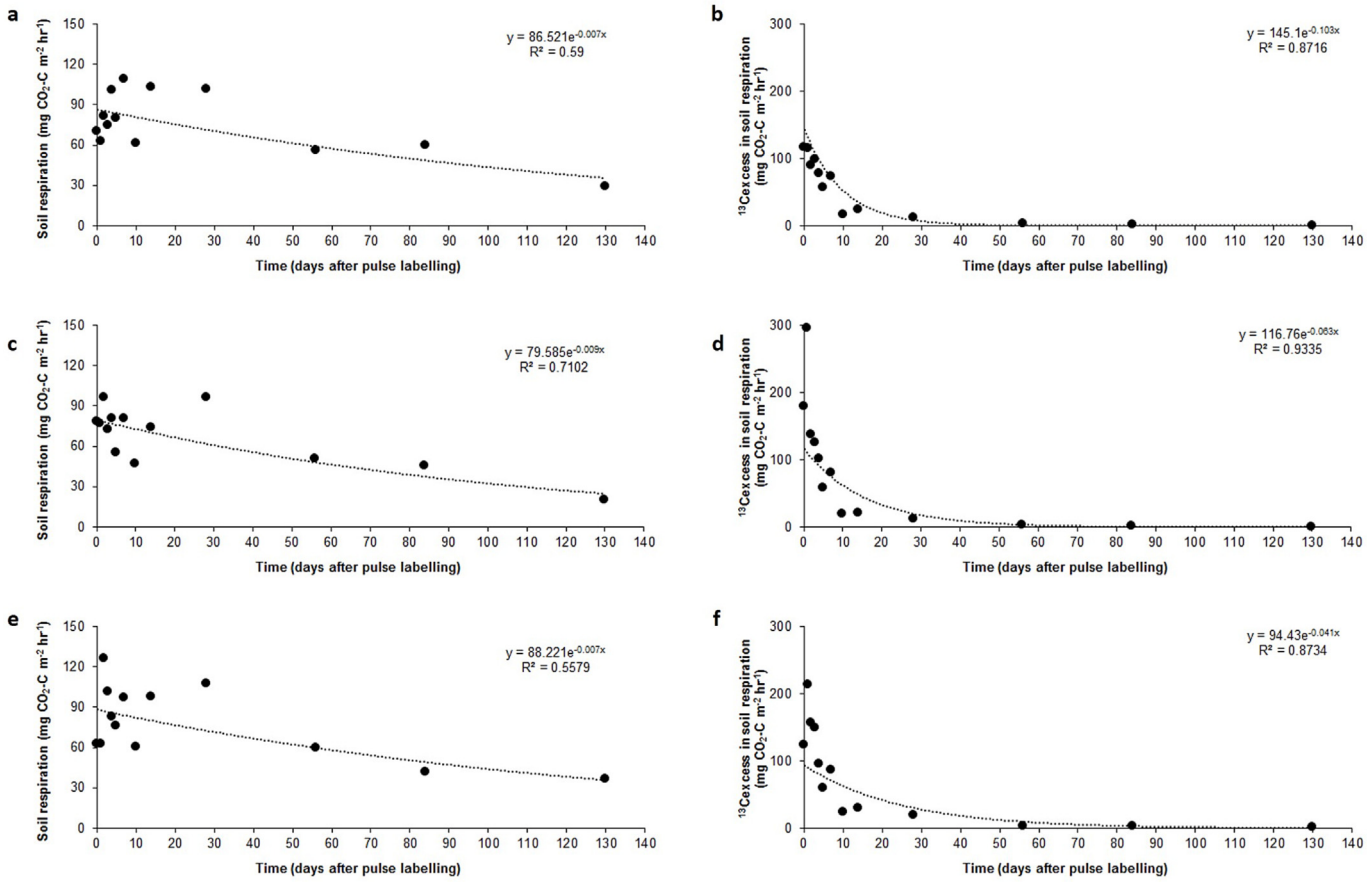

Fig. 2. Exponential fitted time course of soil respiration (a, c, e) and excess ^{13}C flux in soil respiration (b, d, f) in three *Miscanthus* species across the 130 day sampling period (a-b: *Miscanthus* × *giganteus* (GIG), c–d: *Miscanthus sinensis* (SIN) and e–f: *Miscanthus lutarioriparius* (LUT)).

20–30 cm layer, but the differences with the top layer were only significant for GIG ($ANOVA_{DEPTH}$: $F = 11.16$, $p = 0.0095$ for total C and $ANOVA_{DEPTH}$: $F = 7.97$, $p = 0.0205$ for total N; Figs. 1c,d).

Natural abundance carbon delta values of the plant samples clearly indicated the use of C_4 carbon fixation by the three *Miscanthus* species, with values ranging from −9.45 to −13.73 (Table 1). However, very little of this enriched plant material has been incorporated into the C_3 soils since the start of the field trial, as indicated by the low isotopic values (around −26 ‰) measured after three years and across the three treatments (Table 1). The less negative delta values were measured in the GIG soils, with the deepest soil horizon also showing the highest isotopic enrichment (Table 1).

3.2. Influence of Miscanthus species on soil respiration and ^{13}C excess rates

Soil respiration rates for all three *Miscanthus* treatments steadily declined as the growing season ended (Repeated Measures of ANOVA, Wilk's Lambda test: $F_{TIME} = 6.26$, $p = 0.0184$; Fig. 2), but no significant differences in these temporal trends were observed between species during the post-pulse period (Repeated Measures of ANOVA, Wilk's Lambda test: $F_{TIME*SPECIES} = 1.10$, $p = 0.4439$). Abiotic conditions were the main drivers behind overall soil respiration rates, with warmer temperatures (soil and air temperatures) having a significant positive effect on C fluxes (Pearson correlation, $p = 0.0002$, and $p < 0.0001$, respectively) and soil moisture having the opposite effect ($p = 0.0240$).

However, the response of soil respiration to changes in temperature and moisture regimes was significantly different between *Miscanthus* species (Table 2), and while C fluxes from GIG and LUT were unaffected by soil moisture, this abiotic factor had a significant influence on the amount of CO_2 emitted from SIN soils (Table 2). Across the whole study period, the soils of the SIN plots had, on average, a higher moisture content than those under the other two crops (albeit the differences were only significant with the LUT plots; Table 3), and with the majority of the soil samples exceeding the value of 30 % (Fig. S3). The negative effect of a higher soil moisture content on soil respiration rates have likely mitigated the stimulating effects of temperature and resulted in the lowest amounts of CO_2 being released from the SIN soils (Post-pulse measurements, Table 3).

The highest ^{13}C enrichment flux (Fig. 2) was observed during the first 24 h following the ^{13}C pulse in all three species. Thereafter ^{13}C effluxes decreased very rapidly and 3 days after pulse-labelling ca. 50 % of the tracer was lost, with the rest being gradually respired during the next 25 days (Repeated Measures of ANOVA, Wilk's Lambda test: $F_{TIME} = 110.48$,

Table 2
Spearman correlation coefficients and significance relating soil respiration rates and amount of excess ^{13}C in soil respiration to abiotic variables in three *Miscanthus* species.

	Miscanthus × *giganteus*		*Miscanthus sinensis*		*Miscanthus lutarioriparius*	
	r	p	r	p	r	p
Soil respiration						
Air temperature	0.38154	0.0198	0.38385	0.0208	0.49463	0.0025
Soil temperature	0.37644	0.0217	0.25948	0.1265	0.47701	0.0038
Soil moisture	−0.19905	0.0806	−0.24568	0.0349	0.00028	0.9856
^{13}C excess						
Air temperature	0.67580	<0.0001	0.57243	0.0003	0.74725	<0.0001
Soil temperature	0.69608	<0.0001	0.59742	<0.0001	0.78398	<0.0001
Soil moisture	−0.51394	<0.0001	−0.61630	<0.0001	−0.55615	<0.0001

Table 3
Averaged pulse-chambers measurements one week before and across the whole pulse-labelling experiment of abiotic conditions, soil respiration, $^{13}CO_2$ excess, and chemical properties, delta values of above and belowground vegetation and soils (rhizospheric and bulk soil) per *Miscanthus* species (mean ± S.E.; n = 3). Different letters indicate significant differences between *Miscanthus* species per parameter.

	Miscanthus × *giganteus*	*Miscanthus sinensis*	*Miscanthus lutarioriparius*
Pre-pulse measurements (one week prior to pulse)			
Air temperature (°C)	27.93 ± 0.75a	27.47 ± 0.53a	28.63 ± 0.64a
Soil temperature (°C)	17.77 ± 0.12a	17.90 ± 0.23a	18.27 ± 0.09a
Soil moisture (%)	18.87 ± 1.61ab	20.36 ± 0.78a	14.69 ± 1.41b
Standing biomass (g/m^2)	2849 ± 368a	3543 ± 470a	5081 ± 973a
Soil respiration (mg CO_2- C m^2 h^{-1})	104.79 ± 12.38a	123.61 ± 10.84a	93.98 ± 10.84a
Post-pulse measurements			
Air temperature (°C)	19.51 ± 0.67a	19.47 ± 0.66a	19.63 ± 0.64a
Soil temperature (°C)	16.31 ± 0.43a	16.41 ± 0.43a	16.59 ± 0.44a
Soil moisture (%)	30.08 ± 0.82ab	32.77 ± 0.88a	29.79 ± 1.02b
Soil respiration (mg CO_2-C m^{-2} h^{-1})	75.98 ± 4.23a	69.42 ± 3.56a	79.83 ± 4.88a
$^{13}CO_2$ excess (CO_2-^{13}C m^{-2} h^{-1})	52.48 ± 6.22a	83.89 ± 12.72a	77.08 ± 9.81a
Vegetation			
Leaves C content (%)	43.37 ± 0.28a	43.80 ± 0.15ab	44.19 ± 0.22b
Stems C content (%)	43.63 ± 0.21a	43.88 ± 0.21a	44.10 ± 0.27a
Rhizomes C content (%)	40.98 ± 0.49a	39.68 ± 0.90a	38.18 ± 1.39a
Roots C content (%)	29.19 ± 1.27a	28.11 ± 1.20a	30.58 ± 1.29a
Leaves N content (%)	1.58 ± 0.09ab	1.32 ± 0.08a	1.83 ± 0.10b
Stems N content (%)	0.83 ± 0.10a	0.76 ± 0.07a	0.79 ± 0.10a
Rhizomes N content (%)	0.98 ± 0.04a	0.82 ± 0.04a	0.90 ± 0.07a
Roots N content (%)	0.70 ± 0.03a	0.71 ± 0.03a	0.81 ± 0.03b
$\delta^{13}C$ leaves (‰)	97.70 ± 13.64a	100.37 ± 15.36a	78.70 ± 17.41a
$\delta^{13}C$ stems (‰)	114.94 ± 10.21a	120.16 ± 9.94a	72.22 ± 7.86b
$\delta^{13}C$ rhizomes (‰)	38.35 ± 10.86ab	64.01 ± 9.36a	30.98 ± 6.26b
$\delta^{13}C$ roots (‰)	4.38 ± 2.85a	14.59 ± 3.20b	4.65 ± 2.52a
Rhizosoil			
Total C content (%)	3.84 ± 0.11a	3.96 ± 0.09ab	4.40 ± 0.18b
Total N content (%)	0.37 ± 0.01a	0.37 ± 0.01ab	0.40 ± 0.01b
$\delta^{13}C$ (‰)	−24.99 ± 0.21a	−23.92 ± 0.37b	−24.53 ± 0.29ab
Soil			
Total C content 0–30 cm (%)	3.13 ± 0.06a	3.38 ± 0.06b	3.54 ± 0.08b
Total C content 0–10 cm (%)	3.34 ± 0.07a	3.54 ± 0.07ab	3.65 ± 0.11b
Total C content 10–20 cm (%)	3.32 ± 0.09a	3.55 ± 0.08ab	3.87 ± 0.14b
Total C content 20–30 cm (%)	2.74 ± 0.09a	3.14 ± 0.11b	3.09 ± 0.11ab
Total N content 0–30 cm (%)	0.32 ± 0.01a	0.37 ± 0.03b	0.35 ± 0.01b
Total N content 0–10 cm (%)	0.33 ± 0.01a	0.35 ± 0.01a	0.35 ± 0.01a
Total N content 10–20 cm (%)	0.34 ± 0.01a	0.36 ± 0.01ab	0.38 ± 0.01b
Total N content 20–30 cm (%)	0.29 ± 0.01a	0.32 ± 0.01a	0.31 ± 0.01a
$\delta^{13}C$ 0–30 cm (‰)	−26.91 ± 0.06a	−26.58 ± 0.09b	−26.44 ± 0.08b
$\delta^{13}C$ 0–10 cm (‰)	−26.69 ± 0.10a	−26.21 ± 0.15b	−26.10 ± 0.15b
$\delta^{13}C$ 10–20 cm (‰)	−27.21 ± 0.10a	−26.96 ± 0.13a	−26.82 ± 0.10a
$\delta^{13}C$ 20–30 cm (‰)	−26.84 ± 0.11a	−26.58 ± 0.13ab	−26.40 ± 0.15b

$p < 0.0001$; Fig. 2). Despite respiring less CO_2, the SIN soils emitted a greater proportion of the heavier isotope into the atmosphere when compared to the other two species, although the differences were not significant (Table 3). Cumulative values of $^{13}CO_2$ excess in SIN, LUT and GIG for 130 days were 1035 ± 131, 964 ± 52 and 682 ± 134 mg CO_2-C m^{-2} h^{-1}, respectively.

3.3. Influence of Miscanthus species on the allocation of recently photosynthetised ^{13}C carbon in plant tissues

Pulse labelling with $^{13}CO_2$ resulted in a rapid isotopic enrichment of the vegetation and within the first 4 h the amount of ^{13}C fixed into plant biomass (as mg C m^{-2}) was higher on average, albeit not significant, in the GIG and SIN plants than those in the LUT plots ($ANOVA_{SPECIES}$: $F = 0.81$, $p = 0.4582$; Fig. 3) and inversely related to their respective standing biomass prior to pulse-labelling (Table 3 and Fig. 3).

Furthermore, across the whole investigated period, more recent C assimilates (as ^{13}C excess) were allocated aboveground than in the belowground biomass ($ANOVA_{TISSUE}$: $F = 54.44$, $p < 0.0001$) and with species identity having a significant influence on the amounts of ^{13}C assimilated by the different plant tissues, with the exception of the leaves (Table 4). Accordingly, GIG and LUT incorporated 77.7 % and 73.8 %, respectively, of the total amount of ^{13}C fixed in the stems compared to SIN (69.3 %), but the latter showed a greater isotopic enrichment in the rhizomes and roots (22 % and 8 % on average, respectively). GIG incorporated 16.3 % and 6.0 % and LUT 18.0 % and 7.3 % of total ^{13}C fixed into rhizomes and roots, respectively.

In the three species, enrichment within the upper leaves peaked between 4 and 24 h following ^{13}C addition (Fig. 4a–c and Table 5), with the rest of the leaves and stems peaking between 24 h to 3 days post ^{13}C labelling (Fig. 4d–f and Table 5). Rhizome enrichment peaked between 1 and 14 days (Fig. 4g–I and Table 5), and the root enrichment between 3 and 56 days (Fig. 4j–l and Table 5), highlighting the time-lag between fixing of current photosynthate in the leaves and subsequent transport and re-allocation in other plant tissues. Thereafter, enrichment levels gradually decreased over the sampling period across the three species (Repeated Measures of ANOVA, Wilk's Lambda test: $F_{TIME} = 5.54$, $p = 0.0015$ and $F_{TIME*SPECIES} = 0.87$, $p = 0.6107$; Fig. 4), although more slowly in the case of the stems in all three species, with 13–27 % of the maximum enrichment still remaining in this plant section 190 days after pulse-labelling (Fig. 4). The only significant time × species interaction was observed for rhizomes (Table 5), and indicated that not only were SIN rhizomes significantly enriched compared to the other two *Miscanthus* species on three sampling occasions (24 h, 3 days and 56 days), but also a different turnover rate

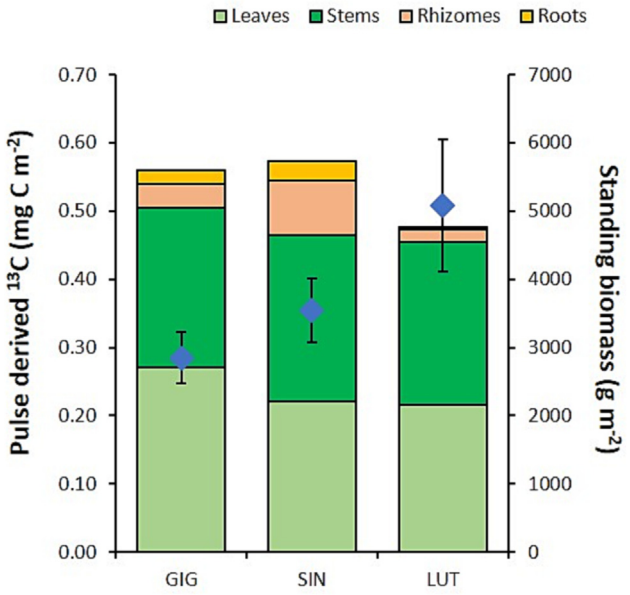

Fig. 3. Relative amount of ^{13}C fixed (as pulse-derived ^{13}C per m^2) into the different plant tissues (i.e., leaves, stems, rhizomes and roots; stacked columns and primary axis) at the first sampling (4 h) and the average standing biomass (g/m^2) of each *Miscanthus* species (*Miscanthus* × *giganteus* (GIG), *Miscanthus sinensis* (SIN) and *Miscanthus lutarioriparius* (LUT)) in the pulse-chamber on the week before pulse-labelling (blue diamonds and secondary axis).

of recently assimilated C in this plant section compared to the other two species. Thus, while the small amounts of ^{13}C assimilated by GIG became fixed and stored in this plant tissue after 24 h and in LUT they were rapidly lost (as evidenced by the higher value of the slope of the exponential curve), a more progressive decline over time was observed in the case of SIN rhizomes, which led to similar amounts of labelled C remaining (relative to maximum enrichment) for both GIG and SIN at the end of the experimental study (Fig. 4).

Compared to plant tissues, only small amounts of recently photosynthesised ^{13}C carbon were incorporated into the soils under the three crops (<1 % compared to the total amount fixed in the plants). However, despite the low ^{13}C translocation belowground, species identity had a significant effect on the averaged enrichments of both rhizospheric and bulk soils (Table 4) as these two soil pools were significantly more enriched under SIN and LUT than under GIG (Fig. 5). Over the study period, ^{13}C enrichment within the rhizosphere peaked at day 14 for LUT and at day 28 for SIN, whereas no time effect was observed for the ^{13}C enrichment in the bulk soils (Table 5).

4. Discussion

Our study provides support for morphological trait differences in above and below-ground *Miscanthus* species having a significant effect on C allocation and turnover. This is important because the majority of research and modelling predictions has focused on the one species, the sterile allotriploid hybrid *M.* × *giganteus* and hence, our findings suggest that the careful selection of a particular species could help to improve the soil C sink function and the net GHG mitigation or removal potential of this perennial bioenergy production system.

4.1. Growing Miscanthus for biomass production

It has been suggested that plant height, rather than shoot density, can be used as an index of aboveground yield (Clifton-Brown et al., 2001) and that a greater ploidy level can improve biomass production (Zub et al., 2011). At our study site, the diploid LUT has the tallest plants, but produced a similar crop yield (and had the highest standing biomass before the start of the

Table 4
Results from ANOVA for C and N contents, delta values and ^{13}C excess (atom %) of above and belowground vegetation, rhizospheric and bulk soils.

	Bulk soil			Rhizosoil			Leaves			Stems			Rhizomes			Roots		
	df	F	p		df	F	p		df	F	p		df	F	p		df	F	p
Carbon (%)				Carbon (%)				Carbon (%)				Carbon (%)				Carbon (%)			
Species	2	9.34	<0.0001	Species	2	4.70	0.0117	Species	2	3.29	0.0423	Species	2	1.1	0.338	Species	2	1.96	0.1465	Species	2	0.97	0.3822
Depth	2	30.34	<0.0001																				
Species × depth	4	0.38	0.8261																				
Nitrogen (%)				*Nitrogen (%)*				*Nitrogen (%)*				*Nitrogen (%)*				*Nitrogen (%)*				*Nitrogen (%)*			
Species	2	3.73	0.0253	Species	2	4.42	0.0150	Species	2	7.66	0.0009	Species	2	0.05	0.9552	Species	2	2.82	0.0651	Species	2	4.87	0.0099
Depth	2	4.02	0.0192																				
Species × depth	4	1.74	0.1409																				
$\delta^{13}C$ (‰)				$\delta^{13}C$ (‰)	2	3.44	0.0369	$\delta^{13}C$ (‰)	2	0.57	0.5669	$\delta^{13}C$ (‰)	2	7.74	0.0008	$\delta^{13}C$ (‰)	2	3.65	0.03	$\delta^{13}C$ (‰)	2	4.11	0.0197
Species	2	10.84	<0.0001	Species				Species				Species				Species				Species			
Depth	2	20.60	<0.0001																				
Species × depth	4	0.34	0.8541																				
^{13}C excess (atom %)				^{13}C excess (atom %)				^{13}C excess (atom %)				^{13}C excess (atom %)				^{13}C excess (atom %)				^{13}C excess (atom %)			
Species	2	50.34	<0.0001	Species	2	7.01	0.0015	Species	2	0.45	0.639	Species	2	6.21	0.003	Species	2	3.54	0.0334	Species	2	3.82	0.0258
Depth	2	0.57	0.5673																				
Species × depth	4	4.56	0.0014																				

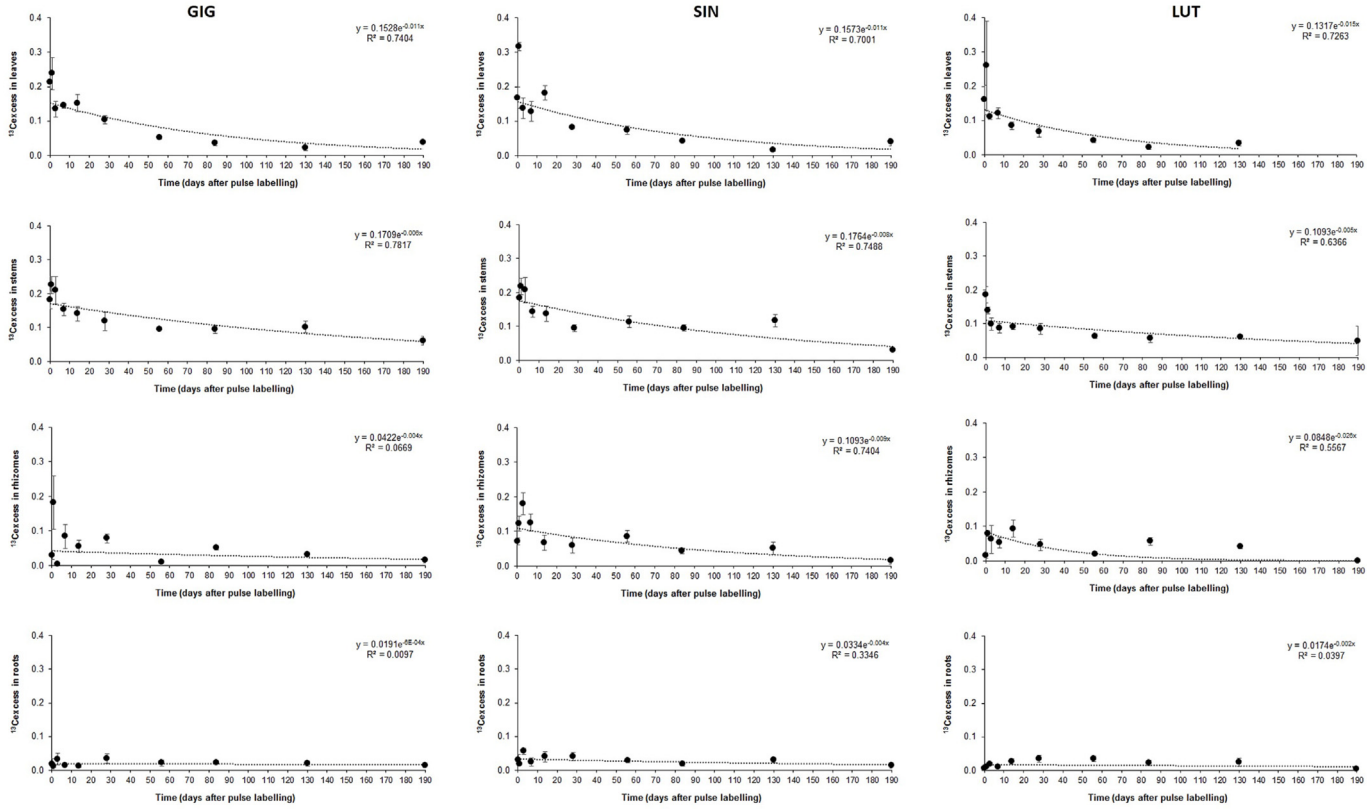

Fig. 4. Exponential fitted time course of pulse-derived ^{13}C incorporation into upper leaves, lower leaves + stems, rhizomes and roots at each *Miscanthus* species (*Miscanthus* × *giganteus* (GIG), *Miscanthus sinensis* (SIN) and *Miscanthus lutarioriparius* (LUT)) across the 190 day sampling period.

pulse-labelling experiment) to the triploid GIG. That GIG is the *Miscanthus* plant with the highest primary productivity in terms of crop yield has been reported in several studies (Lewandowski et al., 2000; Pyter et al., 2007; Li et al., 2018; Fradj et al., 2020), but Clifton-Brown et al. (2001) specifically mentioned LUT (referring to *Miscanthus sacchariflorus lutarioriparius*) as an exception to this general relationship of stem height being the best indicator of yield, due to its low stem density. However, above-ground biomass of *Miscanthus* species and hybrids varies with location, year of cultivation and planting densities (Feng et al., 2015; Clifton-Brown et al., 2019; Shepherd et al., 2020). For example, for mature GIG in England a gradual yield increase with crop age has been recorded, but in stands with low planting densities yields plateau after 9 years (Shepherd et al., 2020). Furthermore, long-term crop performance also depends on genotypic variability, and a field experiment with 15 *Miscanthus* species reported a shorter establishment period to reach a yield plateau of GIG and LUT than of SIN hybrids (Gauder et al., 2012).

A lower crop yield than expected for a taller crop such as LUT could also be likely a consequence of a higher proportion of pre-winter leaf mass dropped by this species (McCalmont et al., in prep). These losses originated from senescent leaves can represent a high percentage of the total above-ground biomass that is produced, with important implications for the total biomass that can be finally harvested (Kahle et al., 2001).

Abscised leaves have seen to contribute more to the soil C accumulation than the rhizomes or roots in *Miscanthus* crops (Amougou et al., 2012). Therefore, it is possible to assume that the significant higher concentration of organic C and total N the soils under LUT is the result of a higher input of leaf litter. The fact that the ^{13}C allocation to bulk soil was higher in LUT relative to GIG and SIN (albeit extremely low), but not different in rhizosphere soils, supports the idea that this ^{13}C return may be coming more from litter rather than root deposition relative to the other species. In addition, and despite the lack of significant differences in the C and N contents of leaves, the higher quality (in terms of C/N ratio) of the LUT litter could also have positive implications for decomposition processes, as it has been seen in previous studies (Yajun et al., 2016; Zhao et al., 2020).

Table 5
Results from Repeated Measures of ANOVA for the effect of *Miscanthus* species on pulse derived ^{13}C allocation in above- and below-ground plant biomass and soils (rhizospheric and bulk soils) over time. Significance multivariate test on each is Wilks' lambda test.

Source	df	Type III SS	Mean square	F Value	Pr > F
Leaves					
Time	8	0.33531531	0.04191	21.5	<0.0001
Time × species	16	0.01846489	0.00115	0.59	0.8743
Stems					
Time	8	0.10290896	0.01286	23.78	<0.0001
Time × species	16	0.01361483	0.00085	1.57	0.1138
Rhizomes					
Time	8	0.03740243	0.00468	4.47	0.0006
Time × species	16	0.03911215	0.00244	2.34	0.0149
Roots					
Time	8	0.00448650	0.00056	2.78	0.0130
Time × species	16	0.00283596	0.00018	0.88	0.5949
Rhizosoil					
Time	8	0.00005037	0.00001	2.67	0.0164
Time × species	16	0.00005338	0.00000	1.41	0.1751
Bulk soil					
Time	8	0.00000205	0.00000026	0.74	0.6570
Time × species	16	0.00000454	0.00000028	0.82	0.6596

4.2. Growing Miscanthus for increased C storage and less CO_2 emissions

Previous studies have shown that, although the three species investigated here show similar performance in radiation capture, GIG exhibits a significantly higher radiation-use efficiency than the noninterspecific

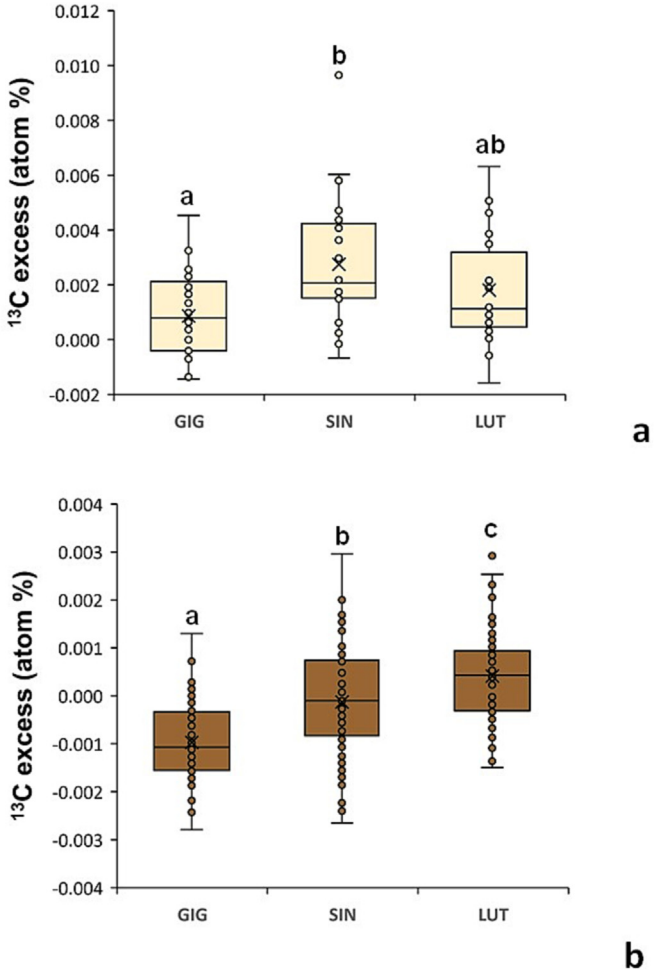

Fig. 5. Box-plots showing the distribution of pulse-derived ^{13}C incorporation into (a) rhizospheric soil and (b) bulk soil under each *Miscanthus* species (pre-pulse). Different letters indicate significant differences between species (*Miscanthus* × *giganteus* (GIG), *Miscanthus sinensis* (SIN) and *Miscanthus lutarioriparius* (LUT)).

hybrid genotypes (Davey et al., 2017). This explains not only the high yields observed in GIG crops, but also its slightly higher incorporation of the ^{13}C tracer into the upper leaves compared to the other two species. Thereafter, enrichment levels decreased in all four plant tissues (upper leaves, stems, rhizomes and roots), but the gradual decrease was less evident in the stems of all three species until the final sampling day. These findings suggest that although three species invest a great proportion of labelled assimilates into photostynthetic biomass (Elias et al., 2017), GIG attains a greater aboveground biomass because they are mostly deposited into cellulose rather than starch (Madison et al., 2017).

There was a small time-lag until this recently assimilated C was transferred to the belowground biomass, in particular in the case LUT, with the ^{13}C enrichment in rhizomes and roots peaking several days later (14 and 28 days, respectively) and the lowest amounts of labelled assimilates being allocated in these two plant sections compared to the other two species (less than a week for translocating higher amounts of assimilates from aboveground biomas to rhizomes and roots in both GIG and SIN). These differences in C transfer and storage could be due to the higher plant height of LUT compared to GIG and SIN and to their different rhizome and root systems. LUT does not form tuft rhizomes (broad and thick-stemmed that creep laterally from where shoots develop) unlike SIN (they do not exhibit the lateral creeping habit and aboveground shoots form dense centralised tufts made out of thinner stems), but those of GIG are an intermediate type (Lewandowski et al., 2003) that creep less than LUT rhizomes (Richter et al., 2015). Tuft type rhizomes yield higher dry matter than the non-tuft types and could explain why, in this study, both GIG and SIN stored more labelled C in their rhizomes than in those of LUT. However, underground production of GIG rhizomes and roots changes during the growing season (Dohleman et al., 2012), and in the case of SIN with spatial location, either in its Japanese native range (reviewed by Stewart et al., 2009) or in cultivations (Christensen et al., 2016). Furthermore, the timing of senescence has been pointed out as critically important for the translocation of mineral nutrients and carbohydrates back to the rhizomes to be remobilised for regrowth in spring (Nunn et al., 2017), which occurs earlier in LUT (McCalmont et al., in prep). Therefore, more research is needed to fully understand the effects of individual species on rhizome C storage dynamics in European *Miscanthus* stands.

Translocation of C from plant tissues into soil respiration occurred very rapidly in the three *Miscanthus* species, before our first measurement (4 h after labelling), in agreement with previous studies (Elias et al., 2017; Robertson et al., 2017a) and the highest ^{13}C enrichment flux was measured during the first 24 h in all three species. Since the rate of transfer from photosynthetic biomass to soil respiration is controlled by phloem transport velocity and environmental conditions (Kuzyakov and Gavrichkova, 2010; Dannoura et al., 2011; Lemoine et al., 2013; Liesche and Patrick, 2017; Gavrichkova and Kuzyakov, 2017), the short time lag observed here can be related to the rapid growth rates of *Miscanthus* spp. that are mainly controlled by temperature (Nunn et al., 2017). Consequently, as expected, soil respiration rates steadily declined as the growing season ended in parallel with decreasing air and soil temperatures and increasing soil moisture levels. Similar seasonal changes in soil respiration rates, with increases in spring and summer and decreases throughout the autumn have been observed in many field studies, including different *Miscanthus* species (Yazaki et al., 2004; Elias et al., 2017; Robertson et al., 2017b). Interestingly, although no significant differences in the rate of transfer of photosynthetically fixed C into respired CO_2 were observed between *Miscanthus* species, SIN translocated more labelled assimilates into soil respiration, but more importantly, under this crop the soils emitted less CO_2 to the atmosphere.

Carbon transfer to soil was negligible and most of the labelled assimilates exudated by the roots remained in the surrounding soil (rhizosphere), specially under SIN and LUT. This contrasts with other studies which found that *Miscanthus*-derived C could represent up to 15–18 % of the total soil C (Christensen et al., 2016) or 26–29 % of the cumulated C input (Hansen et al., 2004), but it is coincidental with other work that reported more variable results depending on duration of the cultivation (Felten and Emmerling, 2012; Al Souki et al., 2021) and soil depth (Felten and Emmerling, 2012; Richter et al., 2015). One possible explanation for these contrasting results is timing of the pulse-labelling, which in our study occurred at the peak of the growing season when plant metabolism and growth of biomass was higher, whereas a later application could have favoured belowground processes. We chose to perform this labeling experiment in mid-summer (late July) because it is the period of maximum biomass accumulation, and consequently, we anticipated a greater belowground transport of non-structural compounds than earlier in the growing season. However, although we acknowledge that our $^{13}CO_2$ pulse-labelling approach might not have induced a measurable amount of labile C into more recalcitrant soil pools (Carbone et al., 2007; Carbone and Trumbore, 2007; Kuzyakov, 2011), it confirmed that after three years since the establishment of the C_3 to C_4 switch trial very low amounts of C_4-derived carbon has been incorporated into the C_3 topsoils.

5. Conclusions

Our study showed that recently photosynthesised C transfer from above-ground vegetation to rhizomes and roots and finally to the soil was rapid (less than two months) in all three *Miscanthus* species. However, more C_4-derived carbon from SIN entered the rhizomes and the roots, and hence susceptible to be retained after the aboveground biomass has been harvested (Robertson et al., 2017a). Therefore, despite being a slow-growing species and having lower above- and below-ground biomass

compared to GIG (Christensen et al., 2016), SIN could be the choice of species to increase C storage in soils, especially in commercial plantations where annual (above-ground) harvesting takes place.

Furthermore, although LUT produces leaf litter of higher quality and had the highest increase in soil C content during the year of study, 25 % of the below-ground biomass of SIN dies off annually (Mun, 1988; Shoji et al., 1990), which could also be decomposed by soil organisms, via bacterial-foodweb driven channels (Elias et al., 2017; Briones et al., 2019). Because *Miscanthus*-derived emissions from senesced biomass or SOM is much slower than from plant metabolic respiration (Robertson et al., 2017a) and our study showed that the soils under SIN emitted less CO_2, this species also shows advantages in terms of climate change mitigation.

Because plant growth and senescence are directly related to abiotic conditions (temperature and soil moisture), the final choice of species for growing *Miscanthus* should also be based on the ability to withstand other environmental stresses in any given agroclimatic area where it is going to be commercially produced (Ouattara et al., 2020). In relation to this, it has been shown that SIN is more resilient to drought and salinity stresses than GIG (Stavridou et al., 2019) and that LUT is much more tolerant to cold winter temperatures than SIN (Yan et al., 2012). Consequently, in the case of Europe, planting LUT is only recommended for those areas with irrigation or no susceptibility to drought, whereas GIG is recommended for most areas of Europe (Lewandowski et al., 2016). However, unlike the sterile hybrid GIG, the two other fertile species (SIN and LUT) can escape from cultivation and have negative effects on nearby resident plant communities (e.g. Quinn et al., 2010; Hager et al., 2015) and hence, developing regionally restricted cultivars to minimize widespread and invasion risks is advocated.

CRediT authorship contribution statement

NPM, JMC and KF planned and designed the research. AM, DMOE and ID performed experiments and conducted fieldwork. MJIB and AM conducted all data analysis. MJIB, NPM, and DMOE wrote the first draft. All authors contributed to the final version of the manuscript.

Data availability

Data will be made available on request.

Declaration of competing interest

The authors declare the following financial interests/personal relationships which may be considered as potential competing interests:

N.P. McNamara, D.M.O. Elias reports financial support was provided by Natural Environment Research Council. K. Farrar, I. Donninson reports financial support was provided by Biotechnology and Biological Sciences Research Council.

Acknowledgements

This work was supported by Energy Technologies Institute (ETI) Ecosystem Land Use Modelling project. NPM and DMOE were also supported by the Natural Environment Research Council award number NE/R016429/1 as part of the UK-SCAPE programme delivering National Capability. Additionally, KF and ID were supported by the Biotechnology and Biological Sciences Council (BBSRC) through the Core Strategic Programme in Resilient Crops: BBS/E/W/0012843A. We thank Kate Rolt, Rebecca Rowe, Rachel Marshall and Jonathan Oxley for field and laboratory support. Authors also acknowledge funding for open access charge from Universidade de Vigo/CISUG.

Appendix A. Supplementary data

Supplementary data to this article can be found online at https://doi.org/10.1016/j.scitotenv.2023.164003.

References

Al Souki, K.S., Burdová, H., Trubač, J., Štojdl, J., Kuráň, P., Kříženecká, S., Machová, I., Kubát, K., Popelka, J., Malinská, H.A., Nebeská, D., Ust'ak, S., Honzík, R., Trögl, J., 2021. Enhanced carbon sequestration in marginal land upon shift towards perennial C_4 *Miscanthus* × *giganteus*: a case study in North-Western Czechia. Agronomy 11, 293. https://doi.org/10.3390/agronomy11020293.

Amougou, N., Bertrand, I., Machet, J.M., Recous, S., 2011. Quality and decomposition in soil of rhizome, root and leaf from *Miscanthus* × *giganteus*, as affected by harvest date and N fertilization. Plant and Soil 338, 83–97. https://doi.org/10.1007/s11104-010-0443-x.

Amougou, N., Bertrand, I., Cadoux, S., Recous, S., 2012. *Miscanthus* × *giganteus* leaf senescence, decomposition and C and N inputs to soil. Glob. Chang. Biol. Bioenergy 4, 698–707. https://doi.org/10.1111/j.1757-1707.2012.01192.x.

Anthony, W.H., Hutchinson, G.L., Livingston, G.P., 1995. Chamber measurement of soil-atmosphere gas-exchange - linear vs. diffusion-based flux models. Soil Sci. Soc. Am. J. 59, 1308–1310. https://doi.org/10.2136/sssaj1995.03615995005900050015x.

Atienza, S.G., Satovic, Z., Petersen, K.K., Dolstra, O., Martín, A., 2002. Preliminary genetic linkage map of *Miscanthus sinensis* with RAPD markers. Theor. Appl. Genet. 105, 946–952. https://doi.org/10.1007/s00122-002-0956-7.

Balslev-Clausen, D., Dahl, T.W., Saad, N., Rosing, M.Y., 2013. Precise and accurate $\delta^{13}C$ analysis of rock samples using Flash Combustion–Cavity Ring Down Laser Spectroscopy. J. Anal. At. Spectrom 28, 516–523. doi: https://doi.org/10.1039/c2ja30240c.

Briones, M.J.I., Elias, D.M.O., Grant, H.K., McNamara, N.P., 2019. Plant identity control on soil food web structure and C transfers under perennial bioenergy plantations. Soil Biol. Biochem. 138, 107603. https://doi.org/10.1016/j.soilbio.2019.107603.

Carbone, M.S., Trumbore, S.E., 2007. Contribution of new photosynthetic assimilates to respiration by perennial grasses and shrubs: residence times and allocation patterns. New Phytol. 176, 124–135. https://doi.org/10.1111/j.1469-8137.2007.02153.x.

Carbone, M.S., Czimczik, C.I., McDuffee, K.E., Trumbore, S.E., 2007. Allocation and residence time of photosynthetic products in a boreal forest using a low-level ^{14}C pulse-chase labeling technique. Glob. Chang. Biol. 13, 466–477. https://doi.org/10.1111/j.1365-2486.2006.01300.x.

Case, S.D.C., McNamara, N.P., Reay, D.S., Whitaker, J., 2012. The effect of biochar addition on N_2O and CO_2 emissions from a sandy loam soil - the role of soil aeration. Soil Biol. Biochem. 51, 125–134. https://doi.org/10.1016/j.soilbio.2012.03.017.

Cattaneo, F., Barbanti, L., Gioacchini, P., Ciavatta, C., Marzador, C., 2014. ^{13}C abundance shows effective soil carbon sequestration in *Miscanthus* and giant reed compared to arable crops under Mediterranean climate. Biol. Fertil. Soils 50, 1121–1128. https://doi.org/10.1007/s00374-014-0931-x.

Chae, W.B., Hong, S.J., Gifford, J.M., Rayburn, A.L., Sacks, E.J., Juvik, J.A., 2014. Plant morphology, genome size, and SSR markers differentiate five distinct taxonomic groups among accessions in the genus *Miscanthus*. Glob. Chang. Biol. Bioenergy 6, 646–660. https://doi.org/10.1111/gcbb.12101.

Christensen, B.T., Laerke, P.E., Jorgensen, U., Kandel, T.P., Thomsen, I.K., 2016. Storage of *Miscanthus*-derived carbon in rhizomes, roots and soil. Can. J. Soil Sci. 96, 354–360. https://doi.org/10.1139/cjss-2015-0135.

Clifton-Brown, J.C., Lewandowski, I., Andersson, B., Basch, G., Christian, D.G., Kjeldsen, J.B., Jørgensen, U., Mortensen, J.V., Riche, A.B., Schwarz, K.-U., Tayebi, K., Teixeira, F., 2001. Performance of 15 *Miscanthus* genotypes at five sites in Europe. Agron. J. 93, 1013–1019. https://doi.org/10.2134/agronj2001.9351013x.

Clifton-Brown, J.C., Breuer, J., Jones, M.B., 2007. Carbon mitigation by the energy crop, *Miscanthus*. Glob. Chang. Biol. 13, 2296–2307. https://doi.org/10.1111/j.1365-2486.2007.01438.x.

Clifton-Brown, J.C., Robson, P.R.H., Allison, G.G., Lister, S.J., Sanderson, R., Morris, C., Hodgson, E., Farrar, K., Hawkins, S., Jensen, E.F., Jones, S.T., Huang, L., Roberts, P.C., Youell, S.J., Jones, B.R., Wright, A., Valentine, J., Donnison, I.S., 2008. *Miscanthus*: breeding our way to a better future. In: Booth, E., Green, M., Karp, A., Shield, I., Stock, D., Turley, D. (Eds.), Aspects of Applied Biology 90, Biomass and Energy Crops III. Sand Hutton, Biomass and Energy Crops III conference, pp. 199–206.

Clifton-Brown, J., Hastings, A., Mos, M., Mccalmont, J.P., Ashman, C., Awty-Carroll, D., Cerazy, J., Chiang, Y.C., Cosentino, S., Cracroft-Eley, W., et al., 2017. Progress in upscaling *Miscanthus* biomass production for the European bio-economy with seed-based hybrids. Glob. Chang. Biol. Bioenergy 9, 6–17. https://doi.org/10.1111/gcbb.12357.

Clifton-Brown, J., Schwarz, K.-U., Awty-Carroll, D., Iurato, A., Meyer, H., Greef, J., Gwyn, J., Mos, M., Ashman, C., Hayes, C., Huang, L., Norris, J., Rodgers, C., Scordia, D., Shafiei, R., Squance, M., Swaller, T., Youell, S., Cosentino, S., Flavell, R., Donnison, I., Robson, P., 2019. Breeding strategies to improve *Miscanthus* as a sustainable source of biomass for bioenergy and biorenewable products. Agronomy 9, 673. https://doi.org/10.3390/agronomy9110673.

Cosentino, S.L., Patane, C., Sanzone, E., Copani, V., Foti, S., 2007. Effects of soil water content and nitrogen supply on the productivity of *Miscanthus* × *giganteus* Greef et Deu. in a Mediterranean environment. Indust. Crops Products 25, 75–88. https://doi.org/10.1016/j.indcrop.2006.07.006.

Dannoura, M., Maillard, P., Fresneau, C., Plain, C., Berveiller, D., Gerant, D., Chipeaux, C., Bosc, A., Ngao, J., Damesin, C., Loustau, D., Epron, D., 2011. In situ assessment of the velocity of carbon transfer by tracing ^{13}C in trunk CO_2 efflux after pulse labelling: variations among tree species and seasons. New Phytol. 190, 181–192. https://doi.org/10.1111/j.1469-8137.2010.03599.x.

Davey, C., Jones, L., Squance, M., Purdy, S., Maddison, A., Cunniff, J., Donnison, I., Clifton-Brown, J., 2017. Radiation capture and conversion efficiencies of *Miscanthus sacchariflorus*, *M. sinensis* and their naturally occurring hybrid *M.* × *giganteus*. Glob. Chang. Biol. Bioenergy 9, 385–399. https://doi.org/10.1111/gcbb.12331.

Dohleman, F.G., Heaton, E.A., Arundale, R.A., Long, S.P., 2012. Seasonal dynamics of above- and below-ground biomass and nitrogen partitioning in *Miscanthus* × *giganteus* and

Panicum virgatum across three growing seasons. Glob. Chang. Biol. Bioenergy 4, 534–544. https://doi.org/10.1111/j.1757-1707.2011.01153.x.

Dondini, M., van Groeningen, K.J., del Galdo, I., Jones, M.B., 2009. Carbon sequestration under *Miscanthus*: a study of ^{13}C distribution in soil aggregates. Glob. Chang. Biol. Bioenergy 1, 321–330. https://doi.org/10.1111/j.1757-1707.2009.01025.x.

Drewer, J., Finch, J.W., Lloyd, C.R., Baggs, E.M., Skiba, U., 2012. How do soil emissions of N_2O, CH_4 and CO_2 from perennial bioenergy crops differ from arable annual crops? Glob. Chang. Biol. Bioenergy 4, 408–419. https://doi.org/10.1111/j.1757-1707.2011.01136.x.

Dufossé, K., Drewer, J., Gabrielle, B., Drouet, J.-L., 2014. Effects of a 20-year old *Miscanthus* × *giganteus* stand and its removal on soil characteristics and greenhouse gas emissions. Biomass Bioenergy 69, 198–210. https://doi.org/10.1016/j.biombioe.2014.07.003.

Elias, D.M.O., Rowe, R.L., Pereira, M.G., Stott, A.W., Barnes, C.J., Bending, G.D., McNamara, N.P., 2017. Functional differences in the microbial processing of recent assimilates under two contrasting perennial bioenergy plantations. Soil Biol. Biochem. 114, 248–262. https://doi.org/10.1016/j.soilbio.2017.07.026.

Felten, D., Emmerling, C., 2012. Accumulation of *Miscanthus*-derived carbon in soils in relation to soil depth and duration of land use under commercial farming conditions. J. Plant Nutr. Soil Sci. 175, 661–670. https://doi.org/10.1002/jpln.201100250.

Feng, X., He, Y., Fang, J., Fang, Z., Jiang, B., Brancourt-Hulmel, M., Zheng, B., Jiang, D., 2015. Comparison of the growth and biomass production of *Miscanthus sinensis*, *Miscanthus floridulus* and *Saccharum arundinaceum*. Span. J. Agric. Res. 13, e0703. https://doi.org/10.5424/sjar/2015133-7262.

Feng, H., Lin, C., Liu, W., Xiao, L., Zhao, X., Kang, L., Liu, X., Sang, T., Yi, Z., Yan, J., Huang, H., 2022. Transcriptomic characterization of *Miscanthus sacchariflorus* × *M. lutarioriparius* and its implications for energy crop development in the semiarid mine area. Plants (Basel) 11 (12), 1568. https://doi.org/10.3390/plants11121568.

Fradj, N.B., Rozakis, S., Borzęcka, M., Matyka, M., 2020. *Miscanthus* in the European bioeconomy: a network analysis. Ind. Crop Prod. 148, 112281. https://doi.org/10.1016/j.indcrop.2020.112281.

Gauder, M., Graeff-Hönninger, S., Lewandowski, I., Claupein, W., 2012. Long-term yield and performance of 15 different *Miscanthus* genotypes in Southwest Germany. Ann. Appl. Biol. 160, 126–136. https://doi.org/10.1111/j.1744-7348.2011.00526.x.

Gavrichkova, O., Kuzyakov, Y., 2017. The above-belowground coupling of the C cycle: fast and slow mechanisms of C transfer for root and rhizomicrobial respiration. Plant and Soil 410, 73–85. https://doi.org/10.1007/s11104-016-2982-2.

Glynn, E., Brennan, J.M., Walsh, E., Feechan, A., McDonnell, K., 2015. The potential of *Miscanthus* to harbour known cereal pathogens. Eur. J. Plant Pathol. 141, 35–44. https://doi.org/10.1007/s10658-014-0519-1.

Greef, J.M., Deuter, M., Jung, C., Schondelmaier, J., 1997. Genetic diversity of European *Miscanthus* species revealed by AFLP fingerprinting. Genet. Resour. Crop. Evol. 44, 185–195. https://doi.org/10.1023/A:1008693214629.

Hager, H.A., Rupert, R., Quinn, L.D., Newman, J.A., 2015. Escaped *Miscanthus sacchariflorus* reduces the richness and diversity of vegetation and the soil seed bank. Biol. Invasions 17, 1833–1847. https://doi.org/10.1007/s10530-014-0839-2.

Hansen, E.M., Christensen, B.T., Jensen, L.S., Kristensen, K., 2004. Carbon sequestration in soil beneath long-term *Miscanthus* plantations as determined by ^{13}C abundance. Biomass Bioenergy 26, 97–105. https://doi.org/10.1016/S0961-9534(03)00102-8.

Hastings, A., Clifton-Brown, J., Wattenbach, M., Mitchell, C.P., Stampfl, P., Smith, P., 2009. Future energy potential of *Miscanthus* in Europe. Glob. Chang. Biol. Bioenergy 1, 180–196. https://doi.org/10.1111/j.1757-1707.2009.01012.x.

Hillier, J., Whittaker, C., Dailey, G., Aylott, M., Casella, E., Richter, G.M., Riche, A., Murphy, R., Taylor, G., Smith, P., 2009. Greenhouse gas emissions from four bioenergy crops in England and Wales: integrating spatial estimates of yield and soil carbon balance in life cycle analyses. Glob. Chang. Biol. Bioenergy 1, 267–281. https://doi.org/10.1111/j.1757-1707.2009.01021.x.

Hodkinson, T.R., Chase, M.W., Renvoize, S.A., 2002. Characterization of a genetic resource collection for *Miscanthus* (Saccharinae, Andropogoneae, Poaceae) using AFLP and ISSR PCR. Ann. Bot. 89, 627–636. https://doi.org/10.1093/aob/mcf091.

Holder, A.J., Clifton-Brown, J., Rowe, R., Robson, P., Elias, D.M.O., Dondini, M., McNamara, N.P., Donnison, I.S., McCalmont, J.P., 2019. Measured and modelled effect of land-use change from temperate grassland to *Miscanthus* on soil carbon stocks after 12 years. Glob. Chang. Biol. Bioenergy 11, 1173–1186. https://doi.org/10.1111/gcbb.12624.

Jensen, E., Farrar, K., Thomas-Jones, S., Hastings, A., Donnison, I.S., Clifton-Brown, J., 2011. Characterization of flowering time diversity in *Miscanthus* species. Glob. Chang. Biol. Bioenergy 3, 387–400. https://doi.org/10.1111/j.1757-1707.2011.01097.x.

Kahle, P., Beuch, S., Boelcke, B., Leinweber, P., Schulten, H.R., 2001. Cropping of *Miscanthus* in Central Europe: biomass production and influence on nutrients and soil organic matter. Eur. J. Agron. 15, 171–184. https://doi.org/10.1016/S1161-0301(01)00102-2.

Katsuno, K., Miyairi, Y., Tamura, K., Matsuzaki, H., Fukuda, K., 2010. A study of the carbon dynamics of Japanese grassland and forest using ^{14}C and ^{13}C. Nucl. Instrum. Methods Phys. Res., Sect. B 268, 1106–1109. https://doi.org/10.1016/j.nimb.2009.10.110.

Kuzyakov, Y., 2011. How to link soil C pools with CO_2 fluxes? Biogeosciences 8, 1523–1537. https://doi.org/10.5194/bg-8-1523-2011.

Kuzyakov, Y., Domanski, G., 2000. Carbon input by plants into the soil. Review. J. Plant Nutr. Soil Sci. 163, 421–431. https://doi.org/10.1002/1522-2624(200008)163:4<421::AID-JPLN421>3.0.CO;2-R.

Kuzyakov, Y., Gavrichkova, O., 2010. REVIEW: time lag between photosynthesis and carbon dioxide efflux from soil: a review of mechanisms and controls. Glob. Chang. Biol. 16, 3386–3406. https://doi.org/10.1111/j.1365-2486.2010.02179.x.

Lemoine, R., La Camera, S., Atanassova, R., Dédaldéchamp, F., Allario, T., Pourtau, N., Bonnemain, J.-L., Laloi, M., Coutos-Thévenot, P., Maurousset, L., Faucher, M., Girousse, C., Lemonnier, P., Parrilla, J., Durand, M., 2013. Source-to-sink transport of sugar and regulation by environmental factors. Front. Plant Sci. 4, 272. https://doi.org/10.3389/fpls.2013.00272.

Lewandowski, I., Clifton-Brown, J., Scurlock, J.M.O., Huisman, W., 2000. *Miscanthus*: European experience with a novel energy crop. Biomass Bioenergy 19, 209–227. https://doi.org/10.1016/S0961-9534(00)00032-5.

Lewandowski, I., Scurlock, J.M.O., Lindvall, E., Christou, M., 2003. The development and current status of perennial rhizomatous grasses as energy crops in the US and Europe. Biomass Bioenergy 25, 335–361. https://doi.org/10.1016/S0961-9534(03)00030-8.

Lewandowski, I., Clifton-Brown, J., Trindade, L.M., van der Linden, G.C., Schwarz, K.-U., Müller-Sämann, K., Anisimov, A., Chen, C.-L., Dolstra, O., Donnison, I.S., Farrar, K., Fonteyne, S., Harding, G., Hastings, A., Huxley, L.M., Iqbal, Y., Khokhlov, N., Kiesel, A., Lootens, P., Meyer, H., Mos, M., Muylle, H., Nunn, C., Özgüven, M., Roldán-Ruiz, I., Schüle, H., Tarakanov, I., van der Weijde, T., Wagner, M., Xi, Q., Kalinina, O., 2016. Progress on optimizing *Miscanthus* biomass production for the European bioeconomy: results of the EU FP7 project OPTIMISC. Front. Plant Sci. 7, 1620. https://doi.org/10.3389/fpls.2016.01620.

Li, W., Ciais, P., Makowski, D., Peng, S., 2018. A global yield dataset for major lignocellulosic bioenergy crops based on field measurements. Scientific Data 5. https://doi.org/10.1038/sdata.2018.169 art. 180169.

Liesche, J., Patrick, J., 2017. An update on phloem transport: a simple bulk flow under complex regulation. F1000Res. 6, 1–12. https://doi.org/10.12688/f1000research.12577.1.

Liu, C., Xiao, L., Jian, J., Wang, W., Gu, F., Song, D., Yi, Z., Jin, Y., Li, L., 2013. Biomass properties from different *Miscanthus* species. Food Energy Security 2, 12–19. https://doi.org/10.1002/fes3.19.

Madison, A.L., Camargo-Rodríguez, A., Scott, I.M., Jones, C.M., Elias, D.M.O., Hawkins, S., Massey, A., Clifton-Brown, J., McNamara, N.P., Donnison, I.S., Purdy, S.J., 2017. Predicting future biomass yield in *Miscanthus* using the carbohydrate metabolic profile as a biomarker. Glob. Chang. Biol. Bioenergy 9, 1264–1278. https://doi.org/10.1111/gcbb.12418.

McCalmont, J.P., Hastings, A., McNamara, N.P., Richter, G.M., Robson, P., Donnison, I.S., Clifton-Brown, J., 2017. Environmental costs and benefits of growing *Miscanthus* for bioenergy in the UK. Glob. Chang. Biol. Bioenergy 9, 489–507. https://doi.org/10.1111/gcbb.12294.

Mun, H.T., 1988. Comparisons of primary production and nutrients absorption by a *Miscanthus sinensis* community in different soils. Plant and Soil 112, 143–149.

Nakajima, T., Yamada, T., Anzoua, K.G., Kokubo, R., Noborio, K., 2018. Carbon sequestration and yield performances of *Miscanthus* × *giganteus* and *Miscanthus sinensis*. Carbon Manag. 9, 415–423. https://doi.org/10.1080/17583 004.2018.1518106.

NSRI, 2008. Soils Site Report. National Soil Resource Institute. Cranfield University, Cranfield.

Nunn, C., Hastings, A.F.S.J., Kalinina, O., Özgüven, M., Schüle, H., Tarakanov, I.G., Van Der Weijde, T., Anisimov, A.A., Iqbal, Y., Kiesel, A., Khokhlov, N.F., McCalmont, J.P., Meyer, H., Mos, M., Schwarz, K.-U., Trindade, L.M., Lewandowski, I., Clifton-Brown, J.C., 2017. Environmental influences on the growing season duration and ripening of diverse *Miscanthus* germplasm grown in six countries. Front. Plant Sci. 8, 907. https://doi.org/10.3389/fpls.2017.00907.

Ouattara, M.S., Laurent, A., Ferchaud, F., Berthou, M., Borujerdi, E., Butier, A., Malvoisin, P., Romelot, D., Loyce, C., 2020. Evolution of soil carbon stocks under *Miscanthus* × *giganteus* and *Miscanthus sinensis* across contrasting environmental conditions. Glob. Chang. Biol. Bioenergy 13, 1–14. https://doi.org/10.1111/gcbb.12760.

Peixoto, M.M., Friesen, P.C., Sage, R.F., 2015. Winter cold-tolerance thresholds in field-grown *Miscanthus* hybrid rhizomes. J. Exp. Bot. 66, 4415–4425. https://doi.org/10.1093/jxb/erv093.

Poeplau, C., Don, A., 2014. Soil C changes under *Miscanthus* driven by C_4 accumulation and C_3 decomposition – toward a default sequestration function. Glob. Chang. Biol. Bioenergy 6, 327–338. https://doi.org/10.1111/gcbb.12043.

Purdy, S.J., Maddison, A.L., Cunniff, J., Donnison, I., Clifton-Brown, J., 2015. Non-structural carbohydrate profiles and ratios between soluble sugars and starch serve as indicators of productivity for a bioenergy grass. AoB Plants 7, lv032. https://doi.org/10.1093/aobpla/plv032.

Pyter, R., Voigt, T.B., Heaton, E.A., Dohleman, F.G., Long, S.P., 2007. Giant *Miscanthus*: biomass crop for Illinois. In: Janick, J., Whipkey, A. (Eds.), Issues in New Crops and New Uses. Ash Press, Norfolk, pp. 39–42.

Quinn, L.D., Allen, D.J., Stewart, R., 2010. Invasiveness potential of *Miscanthus sinensis*: implications for bioenergy production in the United States. Glob. Chang. Biol. Bioenergy 2, 310–320. https://doi.org/10.1111/j.1757-1707.2010.01062.x.

RCEP, 2004. Biomass as a Renewable Energy Source. Royal Commission on Environmental Pollution, London.

Richter, G.M., Agostini, F., Redmile-Gordon, M., White, R., Goulding, K.W.T., 2015. Sequestration of C in soils under *Miscanthus* can be marginal and is affected by genotype-specific root distribution. Agric. Ecosyst. Environ. 200, 169–177. https://doi.org/10.1016/j.agee.2014.11.011.

Robertson, A.D., Davies, C.A., Smith, P., Stott, A.W., Clark, E.L., McNamara, N.P., 2017a. Carbon inputs from *Miscanthus* displace older soil organic carbon without inducing priming. Bioenergy Res. 10, 86–101. https://doi.org/10.1007/s12155-016-9772-9.

Robertson, A.D., Whitaker, J., Morrison, R., Davies, C.A., Smith, P., McNamara, N.P., 2017b. A *Miscanthus* plantation can be carbon neutral without net sequestration in soils. Glob. Chang. Biol. Bioenergy 9, 645–661. https://doi.org/10.1111/gcbb.12397.

Robson, P., Jensen, E., Hawkins, S., White, S.R., Kenobi, K., Clifton-Brown, J., Farrar, K., 2013. Accelerating the domestication of a bioenergy crop: identifying and modelling morphological targets for sustainable yield increase in *Miscanthus*. J. Exp. Bot. 64, 4143–4155. https://doi.org/10.1093/jxb/ert225.

Rowe, R.L., Keith, A.M., Dondini, M., Smith, P., Oxley, J., McNamara, N.P., 2016. Initial soil C and land-use history determine soil C sequestration under perennial bioenergy crops. Glob. Chang. Biol. Bioenergy 8, 1046–1060. https://doi.org/10.1111/gcbb.12311.

Shepherd, A., Clifton-Brown, J., Kam, J., Buckby, S., Hastings, A., 2020. Commercial experience with *Miscanthus* crops: establishment, yields and environmental observations. Glob. Chang. Biol. Bioenergy 12, 510–523. https://doi.org/10.1111/gcbb.12690.

Shoji, S., Kurebyashi, T., Yamada, I., 1990. Growth and chemical composition of Japanese pampas grass (*Miscanthus sinensis*) with special reference to the formation of dark-colored andisols in North-eastern Japan. Soil Sci. Plant Nutr. 36, 105–120. https://doi.org/10.1080/00380768.1990.10415715.

Stavridou, E., Webster, R.J., Robson, P.R.H., 2019. Novel *Miscanthus* genotypes selected for different drought tolerance phenotypes show enhanced tolerance across combinations of salinity and drought treatments. Ann. Bot. 124, 653–674. https://doi.org/10.1093/aob/mcz009.

Stewart, J.R., Toma, Y., Fernandez, F.G., Nishiwakis, A., Yamada, T., Bollero, G., 2009. The ecology and agronomy of *Miscanthus sinensis*, a species important to bioenergy crop development, in its native range in Japan: a review. Glob. Chang. Biol. Bioenergy 1, 126–153. https://doi.org/10.1111/j.1757-1707.2009.01010.x.

Sun, Q., Lin, Q., Yi, Z.-L., Yang, Z.-R., Zhou, F.-S., 2010. A taxonomic revision of *Miscanthus* s.l. (Poaceae) from China. Bot. J. Linn. Soc. 164, 178–220. https://doi.org/10.1111/j.1095-8339.2010.01082.x.

Wagner, M., Mangold, A., Lask, J., Petig, E., Kiesel, A., Lewandowski, I., 2019. Economic and environmental performance of miscanthus cultivated on marginal land for biogas production. Glob. Chang Biol. Bioenergy 11, 34–49. https://doi.org/10.1111/gcbb.12567.

Yajun, X., Yonghong, X., Xinsheng, C., Feng, L., Zhiyong, H., Xu, L., 2016. Non-additive effects of water availability and litter quality on decomposition of litter mixtures. J. Freshwater Ecol. 31, 153–168. https://doi.org/10.1080/02705060.2015.1079559.

Yan, J., Chen, W.-L., Luo, F., Ma, H.-Z., Meng, A.-P., Li, X.-W., Zhu, M., Li, S.-S., Zhou, H.F., Zhu, W.-X., Han, B., Ge, S., Li, J.-Q., Sang, T., 2012. Variability and adaptability of *Miscanthus* species evaluated for energy crop domestication. Glob. Chang. Biol. Bioenergy 4, 49–60. https://doi.org/10.1111/j.1757-1707.2011.01108.x.

Yan, J., Zhu, M.D., Liu, W., Xu, Q., Zhu, C.Y., Li, J.Q., Sang, T., 2016. Genetic variation and bidirectional gene flow in the riparian plant *Miscanthus lutarioriparius*, across its endemic range: implications for adaptive potential. Glob. Chang. Biol. Bioenergy 8, 764–776. https://doi.org/10.1111/gcbb.12278.

Yazaki, Y., Mariko, S., Koizumi, H., 2004. Carbon dynamics and budget in a *Miscanthus sinensis* grassland in Japan. Ecol. Res. 19, 511–520. https://doi.org/10.1111/j.1440-1703.2004.00665.x.

Zatta, A., Clifton-Brown, J., Robson, P., Hasstings, A., Monti, A., 2014. Land use change from C_3 grassland to C_4 *Miscanthus*: effects on SOC and mitigation benefits. Glob. Chang. Biol. Bioenergy 6, 360–370. https://doi.org/10.1111/gcbb.12054.

Zhang, H., Blagodatskaya, E., Wen, Y., Xu, X., Dyckmans, J., Kuzyakov, Y., 2018. Carbon sequestration and turnover in soil under the energy crop *Miscanthus*: repeated ^{13}C natural abundance approach and literature synthesis. Glob. Chang. Biol. Bioenergy 10, 262–271. https://doi.org/10.1111/gcbb.12485.

Zhang, G., Ge, C., Xu, P., Wang, S., Cheng, S., Han, Y., Wang, Y., Zhuang, Y., Hou, X., Yu, T., et al., 2021. The reference genome of *Miscanthus floridulus* illuminates the evolution of Saccharinae. Nature Plants 7, 608–618. https://doi.org/10.1038/s41477-021-00908-y.

Zhao, C.Q., Fan, X.F., Li, X.N., Hou, X.C., Zhang, W.W., Yue, Y.S., Zhu, Y., Wang, C., Zuo, Y.L., Wu, J.Y., 2020. *Miscanthus sacchriflorus* exhibits sustainable yields and ameliorates soil properties but potassium stocks without any input over a 12-year period in China. Glob. Chang. Biol. Bioenergy 12, 556–570. https://doi.org/10.1111/gcbb.12700.

Zimmermann, J., Dauber, J., Jones, M.B., 2012. Soil C sequestration during the establishment phase of *Miscanthus* × *giganteus*: a regional-scale study on commercial farms using ^{13}C natural abundance. Glob. Chang. Biol. Bioenergy 4, 453–461. https://doi.org/10.1111/j.1757-1707.2011.01117.x.

Zub, H.W., Brancourt-Hulmel, M., 2010. Agronomic and physiological performances of different species of *Miscanthus*, a major energy crop. A review. Agronomy for Sustainable Development. 30, pp. 201–214. https://doi.org/10.1051/agro/2009034.

Zub, H.W., Arnoult, S., Brancourt-Hulmel, M., 2011. Key traits for biomass production identified in different *Miscanthus* species at two harvest dates. Biomass Bioenergy 35, 637–651. https://doi.org/10.1016/j.biombioe.2010.10.020.

Zub, H.W., Arnoult, S., Younous, J., Lejeune-Hénaut, I., Brancourt-Hulmel, M., 2012. The frost tolerance of *Miscanthus* at the juvenile stage: differences between clones are influenced by leaf-stage and acclimation. Eur. J. Agron. 36, 32–40. https://doi.org/10.1016/j.eja.2011.08.001.